DOE/ID/13236-4

DEVELOPMENT OF LEAD-FREE COPPER ALLOY-GRAPHITE CASTINGS

P. K. Rohatgi

October 1999

Work Performed Under Contract No. DE-FC07-93ID13236

For
U.S. Department of Energy
Assistant Secretary for
Energy Research
Washington, DC

By
University of Wisconsin-Milwaukee
Milwaukee, WI

DISCLAIMER

DISCLAIMER

Portions of this document may be illegible in electronic image products. Images are produced from the best available original document.

DOE/ID/13236-4

DEVELOPMENT OF LEAD-FREE COPPER ALLOY-GRAPHITE CASTINGS

P. K. Rohatgi

October 1999

Work Performed Under Contract No. DE-FC07-93ID13236

Prepared for the
U.S. Department of Energy
Assistant Secretary for
Energy Research
Washington, DC

Prepared by
University of Wisconsin-Milwaukee
Milwaukee, WI

DEVELOPMENT OF LEAD-FREE COPPER ALLOY-GRAPHITE CASTINGS

Final Report

P. K. Rohatgi
Materials Department
University of Wisconsin-Milwaukee
3200 N. Cramer St.
Milwaukee, WI 53211

Work Performed Under Contract DE-FC07-93ID13236
For the U.S. Department of Energy
Office of Industrial Technologies
Washington, D. C.

DISCLAIMER

ABSTRACT

In this project, graphite is used as a substitute for lead in order to maintain the machinability of plumbing components at the level of leaded brass. To improve the distribution of graphite particles in copper alloys matrix, the following experiments were conducted: water modeling, Flotation, fluidity, and directional solidification experiments. Based on these experiments, a two-stage stirring method for obtaining higher yields, and a more uniform distribution of graphite particles in copper alloys, was developed; in addition the use of Ti was developed as a wetting agent to improve the wettability of graphite in the copper melt. Graphite recoveries were improved observed due to the addition of Ti and the use of optimum mixing technique. In addition, agglomeration of graphite particles was reduced by the addition of aluminum powder.

Graphite dispersed in Cu alloy was observed to impart good machinability and reduce the sizes of chips during machining of plumbing components in a manner similar to lead. Copper alloys containing dispersed graphite particles could be successfully cast in several plumbing fixtures which exhibited acceptable corrosion rate, solderability, platability and pressure tightness. The power consumption for machining of composites was also lower than that of the matrix alloy. In addition, centrifugally cast copper alloy cylinders containing graphite particles were successfully made. Centrifugal casting techniques force graphite particles to be segregated near the inner periphery of centrifugal castings. This leads to centrifugally cast cylinders which have good tribological properties near the inner periphery where graphite particles are segregated. These cylinders can therefore be used for bearing applications, as substitutes for lead containing copper alloys. The results of tribological properties of centrifugally cast copper alloy cylinders containing graphite particles showed that graphite particles improve wear properties. The results indicate that copper graphite alloys developed under DOE project have a great

potential to substitute leaded copper alloys in both plumbing and bearing applications. Graphite is a much lower cost substitute for lead (as compared to Bismuth and Selenium), is nontoxic and available in plenty. The results of this research has been published in fourteen research publications and presented at American Foundrymens Society conferences.

TABLE OF CONTENTS

LIST OF FIGURES

LIST OF TABLES

1. INTRODUCTION

This report summarizes the work undertaken by UWM Foundry Laboratory under the DOE project entitled "Development of Lead-Free Copper Alloy-Graphite Castings". Leaded copper alloys are mainly used for plumbing and bearing applications. Lead remains as discrete soft dispersoids in copper alloy matrix and improves machinability of plumbing components. It does not form a film along grain boundaries, as does bismuth, and is thus not harmful to mechanical properties. Leaching of lead into drinking water from plumbing components may create health hazards. In addition, lead particles and fumes released to the atmosphere during processing of lead containing copper alloys are also a health hazard. Accordingly, the complete substitution of lead in brass plumbing components is of great importance and this project is directed to develop the technology of cast copper-graphite composite castings using standard foundry practices. In addition, in recent years there is need to substitute lead from copper-lead bearing alloys to reduce lead fumes during processing of copper lead bearings.

In this study, graphite is used as a substitute for lead in order to maintain the machinability of plumbing components at the level of leaded brass. Rapid and easy machinability of cast plumbing components is essential to its acceptance. Lead acts as a chip breaker; graphite also does the same. Both lead and graphite provide lubrication and protection against tool wear. Generally, the particles are not wetted by the molten alloys due to the high wetting angles. From thermodynamic view point, the addition of particles into the melt increases the total system energy. Therefore, the particle cannot be easily introduced without any external force. Since graphite is not wetted by molten copper alloys, titanium was developed as a wetting agent to improve the wettability of graphite in the copper melt. Chromium is also known as a good wetting agent for graphite.

However, since Cr_3C_2 is harder than TiC, titanium was selected as a wetting agent for the initial work.

This project was focused on the following: (a) Developing techniques for managing distribution of graphite particles in copper alloy matrix, (b) Flotation phenomena of graphite particles in copper alloy melt, (c) Machinability of copper alloys containing dispersed graphite, (d) Centrifugal casting of copper alloy containing graphite particles, and (e) Tribological properties of centrifugally cast copper alloy containing graphite particles.

Since the density of graphite particles is lower than that of copper alloy, graphite particles float upward, and this causes nonuniform distribution of graphite particles in the matrix. In addition, the final distribution of graphite particles in the matrix depends on the mixing techniques, which determine the distribution and terminal velocity of graphite particles in the matrix. The flotation velocity of graphite particles of different sizes in the melts have been determined. The microstructural observation in the graphite rich zone of gravity casting showed finer grains than in the graphite poor zone. We also developed two-stage mixing techniques to improve the distribution of graphite particles. However, this technique has a tendency to reduce the melt temperature and therefore, a higher melt temperature is necessary to avoid decrease in the melt temperature during mixing. This problem has been resolved by addition of the proper amount of wetting agent titanium, which improves the wettability between graphite and copper alloy melt. An improvement in wettability between graphite particles and the copper alloy melt reduces the required rotational speed of the stirrer and this decreases the amount of porosity in the matrix. Also, the reaction product of TiC, which forms due to the chemical reaction between titanium and graphite, reduces the flotation velocity of graphite particles in the melt owing to the higher density of TiC than graphite. In addition, graphite particles can also be pretreated and

mixed with aluminum powder in order to prevent their agglomeration in the melt.

Since the flotation of graphite particles depends on its particle size, the flotation velocity of agglomerated graphite particles is much higher than that of the non-agglomerated particles. Therefore, it is important to prepare graphite particles, in such a manner that they do not agglomerate, in order to reduce their flotation velocity. For this, graphite particles in selected experiments were mixed with aluminum powders before the addition of the mixture into the melt. It was observed that the distribution of graphite particles in the matrix improved significantly.

The experimental results obtained at UWM showed that graphite dispersed in Cu alloy imparts good machinability to the copper alloys as graphite does in cast iron. Graphite reduces the sizes of chips during machining of plumbing components in a manner similar to lead. In addition, the power consumption for machining the composites was also lower than that of the matrix alloy. Thus graphite can be expected to be a suitable substitute for lead in cast plumbing components.

In addition, we successfully made centrifugally cast copper alloy cylinders containing graphite particles, and determined the processing conditions which provided an optimum microstructure. Since the density of graphite particles is lower than that of copper alloy melt, graphite particles act differently under gravitational and under centrifugal forces. Under gravitational forces, graphite particles tend to float upwards in the melt during holding and during solidification of castings. However, under centrifugal force, graphite particles move towards the inner periphery of centrifugal casting, resulting in a graphite rich zone near the inner periphery where it is required for bearing applications. The problem of flotation of graphite particles in the melt can cause a non uniform distribution of graphite particles in the matrix in

case of slowly cooled gravity castings. However, uniform distribution of graphite can be obtained in thin section sand castings, permanent mold and pressure die castings. Centrifugal casting techniques force graphite particles to be segregated near the inner periphery of centrifugal casting. This results in centrifugal casting which provides good tribological properties near the inner periphery where graphite particles are segregated. The results of tribological properties of centrifugally cast copper alloy containing graphite particles run against cast iron showed that graphite particles reduced friction coefficient, wear rate, and weight loss of the pin. Work has also been completed on tribological properties of centrifugally cast copper graphite alloy running against steel counterface. Our initial results showed the same tendency as observed with the copper graphite alloy pin running against cast iron; graphite particles improve tribological properties of copper alloy. The tribological properties of copper alloy containing graphite particles depend considerably on the formation of graphite layer and the supply of graphite from the matrix, the deformation of the matrix containing graphite or the counterface, and the sustainability of graphite layers on the tribosurface. These influences on tribological properties of copper alloys must be identified. Since the microstructure of centrifugal casting influences tribological properties, more studies on the relationship between processing conditions and tribological properties are required.

The results to date indicate that copper graphite alloys developed under the DOE project have a great potential to substitute leaded copper alloys, both in selected plumbing and bearing applications.

2. WORKSCOPE

To solve the above problems, the University of Wisconsin-Milwaukee has explored the use

of graphite which was found to impart adequate machinability to copper alloys, as it does to cast iron. Based on initial results, graphite was found to impart significant machinability to copper alloys, when properly distributed. Graphite was also found to be acceptable for plumbing applications from the stand point of inertness, platability solderability, pressure tightness and corrosion resistance.

The project was started on January 1, 1994 and finished on June 30, 1999. In the last 5 and half year of the program, primary efforts have been directed towards:

1. Developing techniques for managing distribution of graphite particles in copper alloy matrix.
2. Studies on casting characteristics of copper alloys containing dispersed graphite.
3. Characterization of selected properties of copper alloys containing dispersed graphite.
4. Machinability of copper alloys containing dispersed graphite
5. Centrifugal casting of copper alloys containing graphite particles.
6. Tribological properties of centrifugally cast copper alloy containing graphite particles.

3. Experimental Results and Discussion

3.1 Distribution of Graphite Particles in copper alloy matrix

3.1.1 Water modeling

Because molten copper has a viscosity of 3.6 cP at the melting point, and a lower value at the higher super heat temperature, water with 1 cP viscosity may be used as model fluid.

Model experiments were conducted to determine the effectiveness of the three kinds of stirrers designed and fabricated to improve the quality of suspension of graphite in copper alloys. Three kinds of stirrers having different blade angles, namely, 90 degrees, 60 degrees and 45 degrees, were used for this purpose. At each blade angle, the rpm of the stirrer was varied from 625

to 1500 rpm.

Figure 3.1.1 shows the vortex and bubble formation in water, when a 90-degree angle blade is used at different the speeds. The photograph reveals that a vortex forms at an early stage of rotation at the speed of 625 rpm. It may be observed that water is mixed with heavy turbulence and large amounts of bubbles form at the speed of 750 rpm. The formation of bubbles during mixing has a detrimental effect on the casting. Since the density of the bubble is lower than that of the melt, and their size larger than those of the particles, the flotation velocity of the bubble is faster than that of the particle. With particles preferentially attached to the bubble surface, the presence of bubbles enhances the floatation of particles.

In contrast to the above, a 60-degree blade angle stirrer gives interesting results. Figure 3.1.2 shows the behavior of water when a 60-degree angle blade stirrer is rotated at different speeds. The photographs clearly demonstrate that the vortex will not form at the highest speed of 1250 rpm under the present experimental conditions. In addition, it was observed that even at very high speeds, there was no significant bubble formation in water. A 45-degree angle blade stirrer indicated that up to a speed of 625 rpm there was no vortex or bubble formation, as shown in Fig. 3.1.3. At higher speeds of 1000 rpm and above, there was significant vortex and bubble formation. The present experiments indicate that under the experimental conditions studied, a 60-degree angle blade stirrer performs more efficiently in distributing particles without formation of vortex and air bubbles. This type of 60-degrees stirrer was examined for Stage II in the synthesis of copper graphite composites while 90° was used for Stage I. However, it should be kept in mind that in the actual synthesis of composites, the speed may not be the same as obtained in model experiments since the viscosity of the melts containing dispersed graphite particles will be higher than pure melt and may significantly influence the actual transport phenomena.

3.1.2. Castings Studies

An extensive set of experiments was conducted to determine (1) graphite distribution and (2) the minimum desirable level of titanium to incorporate a known amount of graphite in the liquid metal. To begin with, 0.5%, 1.0% and 1.5% of Ti was added to known amounts of yellow brass (60Cu-40Zn) and C-90300 (Cu88-Sn8-Zn4) along with melts where no Ti was added. A known amount of graphite was added while the melt was being stirred. Table 3.1.1 gives a summary of six samples made to optimize the quantity of wetting agent under one set of conditions. It may be noted that at the 0% titanium level, it was not possible to add any graphite under the present experimental conditions. It is quite evident from the data that the amount of titanium needed, using one-stage stirring, appears to be one half of the amount of graphite to be added into the melt.

Table 3.1.1. Experiments to Optimize Wetting Agent Addition

Sample No.	Alloy	Wetting Agent, Ti wt%	Graphite, wt%	Remarks
1 (DOE 3)	Yellow Brass	0	1.0	Visual observation indicated that there was no graphite getting into the melt after stirring for 30 secs.
2 (DOE 4)	Yellow Brass	0.25	0.42	Addition of graphite powder was stopped the moment graphite was observed on the surface.
3 (DOE 7)	Yellow Brass	0.5	1	It was observed that 0.5% of Ti was just enough to add 1 wt% of graphite.
4 (DOE 8)	Yellow Brass	0.5	1	It is a repetition of DOE 7 to check repeatability.
5 (DOE 9)	Yellow Brass	1	2	It was possible to add 2% graphite with 1% Ti. However, the composite melt was very viscous.
6 (DOE 10)	Yellow Brass	1	2	Repetition of DOE 9.

Chemical analyses of the composite castings were made to determine the amount of graphite along the length of 1 in. diameter 8 in. long castings for various amounts of graphite added in the melt. It is to be recognized, however, that these analyses determine the amount of carbon in the composite and all the carbon may not be in the form of graphite because some of the graphite may form TiC as thin layers on graphite particles, or as separate TiC particles. This type of analysis gives an idea of the actual recovery of graphite and the uniformity in the distribution of graphite along the length of the casting when the melt is stirred only once, without optimization of the relationship between the dimensions of the stirrer and the crucible. For the purpose of chemical analysis, drillings were taken at every one inch interval from the top of the casting, along the longitudinal axis of the casting. Figures 3.1.4 and 3.1.5 show the typical distribution of carbon along the height of the castings in the form of bar charts for castings containing 1% and 2% graphite (targeted percentage). The conclusions drawn are based on several castings. Examination of the figures indicate that even though the targeted weight percentage of graphite in the alloys is varying from 1 to 2%, all the castings exhibit a maximum of 0.27% of carbon. This indicates that under these experimental conditions with a single-stage stirring, the recovery of graphite is very poor. It was observed that recovery of graphite was in the range of 10 to 15% of the targeted percentage. This result shows that in single stage stirring of graphite in copper alloys, the recovery of graphite after solidification was less than satisfactory.

To improve these aspects, graphite was mixed in two stages using a 90 degree angle blade in stage one, and a 60 degree angle blade in stage two. In the first stage, graphite was introduced by creating a high vortex in the liquid melt. This vortex was created to facilitate the easy introduction of graphite into the liquid metal and was necessary due to the four-fold density difference between

graphite particles and the copper melt. During mixing, titanium was added to improve the wettability between the copper melt and graphite particles. In the second stage, the newly designed 60-degree angle blade stirrer was used to uniformly distribute the already introduced graphite inside the liquid, without creating a vortex and bubbles in the melt. The main function of the second stage was to stabilize graphite particles in the melt. Chemical analysis carried out on a 1 inch diameter bar poured under the above mentioned conditions is shown in the form of a bar graph in Fig. 3.1.6. This graph gives the data on castings made under identical experimental conditions but under single-stage stirring, along with the results for two stage stirring. The figure clearly shows that the amount of graphite present in the castings, produced under two-stage stirring, is significantly higher than the graphite present in the castings produced under single-stage stirring. The maximum percentage recovery of graphite in stirring was observed to be about 93%, and the average recovery was about 80 percent. It may be noted from the graph in Fig. 6 that the graphite content from bottom to top is quite uniform for all practical purposes, especially in two-stage stirring. A comparison of the overall recovery of graphite between single-stage stirring and two-stage stirring is illustrated in Fig. 3.1.7. Repeatability of the two stage stirring technique is demonstrated in chemical analysis drillings taken from two castings as shown in Table 3.1.2. While the data are limited, several inferences can be drawn from Table 3.1.2 data as indicated in Table 3.1.3.

With new technologies for deagglomeration of as-received graphite powder which may contain as many as several hundred 5 μm particles in 500 to 800 μm clusters, and properly designed two-stage stirring techniques, it is expected that 80% graphite recovery and uniformity in graphite distribution along the ingot length could be achieved.

Table 3.1.2. An Analysis of Two Castings for Repeatability

Cast No. DOE 20			Cast No. DOE 21		
Drilling Position	**Analyzed Carbon Content %**	**Carbon[a] Recovery %**	**Drilling Position**	**Analyzed Carbon Content %**	**Carbon[a] Recovery %**
Top 1	1.261	90.1	Top 1	1.071	76.5
2	1.307	93.3	2	1.024	73.1
3	1.255	89.6	3	1.094	78.1
4	1.320	94.3	4	1.069	76.4
5	1.183	84.5	5	1.068	76.3
6	0.990	70.7	6	0.849	60.6
7	0.998	71.3	7	1.048	74.9
Bottom 8	0.981	70.1	Bottom 8	1.048	74.9
Average	1.162	83.0	Average	1.033	73.9

[a]Graphite added 1.4 wt%. Additional losses may amount to 2 to 5% of the quantity added.

Table 3.1.3. Some Observations on Table 2 Data

Items	DOE #20	DOE #21
1. Range of maximum variation in graphite content, wt%	0.981 to 1.320 or 0.339	0.849 to 1.094 or 0.245
2. Maximum variation as a fraction of graphite added, %	24	18
3. Maximum variation between the top and bottom graphite levels, wt%	Top 1.261 Bottom 0.981 Difference 0.28	Top 1.07 Bottom 1.048 Difference 0.022
4. Location of minimum graphite level	Bottom	Three inches from the bottom
5. Graphite recovery fraction in the top half of the rod, %	91.8	76.0
6. Overall graphite recovery in DOE #20 and DOE #21 castings.	83.0	73.9

Table 3.1.4. Yellow Brass-Graphite Composite Fluidity-Spiral Evaluation

DOS Sample #	Ti Content, wt%	Graphite Content, wt%	Pouring Temp., °C	Spiral Length, cm
30	0	0	950	15.6
32	0	0	975	24.0
34	1.5	0	960	19.1
35	1.5	1	960	13.6
37	1.5	1.5	960	12.8

3.1.3. Fluidity studies

Suspension of solid particles in liquids is known to increase viscosity and decrease fluidity as well as influence the solidification processes and the casting microstructure of the matrix metal. In

view of this, it is necessary to determine the fluidity and solidification characteristics of copper alloy-graphite composite melt for successful casting of these composites, because that will determine the size and the shape of castings which can be made.

Yellow brass (Cu:60%, Zn:40%) has been used for fluidity tests. The process used for synthesis of the copper-graphite composite involved a two-stage stirring process. The fluidity of the copper-graphite composite alloys was measured by casting fluidity spirals in permanent steel molds following standard foundry procedure. The steel mold was preheated to 260 °C with heating cartridges embedded in the mold. A refractory pouring cup coated with boron nitride was used to maintain velocity and laminar flow of the composite melt in the mold.

A typical copper-graphite composite fluidity spiral is shown in Fig. 3.1.8. The spiral length of the base yellow brass alloy (no Ti) increases by about 60% with an increase in temperature from 950 to 975 °C. At 960 C, with 1.5% Ti, the fluidity decreases with an increase in graphite content, as expected. However, the fluidity of yellow brass containing 1.5% Ti and up to 1.5% graphite remains adequate for making a variety of castings, as indicated from the length of the spirals. At the most, a slightly higher pouring temperature may be required for casting graphite containing yellow brass as compared to conventional yellow brass of the same matrix composition.

3.1.4. Directional Solidification

Directional solidification experiments were conducted to determine the effect of cooling rate on the uniformity of graphite particle distribution and microstructure. As mentioned earlier, a uniform graphite distribution depends on the deagglomeration of graphite particles added to the melt as well as on the as-received graphite condition. In addition, the distribution of graphite

particles is affected by the cooling rate due to the interaction between the growing dendrite arms and graphite particles. When the growing dendrite arms interact with graphite particles, they usually push the graphite particles into the interdendritic regions. Also, the distribution of graphite particles depends on the cooling rate which influences the dendrite arm spacing.

Copper C90300 alloy with 1.5 wt% Gr and 2 wt% Ti was used in this experiment. The change in the temperature of copper melt with time was measured with thermocouples placed in the mold. The thermocouples were connected to a recorder to continuously record the temperature change of the molten metal with time at two locations. The ceramic mold coated with boron nitride wash was preheated to 1500 °C in an electrical resistance furnace. A copper chill was precooled in a freezer at a temperature of –12 °C before setting below the mold and the heat was rapidly extracted vertically downwards.

A typical cooling curve obtained from the bottom and the upper parts of the sample is shown in Fig. 3.1.9. It may be noted that in the initial period, the temperature drop rate (slope) of curve a (mold bottom) is greater than that at the upper part due to the high cooling rate produced by the chill which controls the directional solidification condition. The cooling curves show that at the bottom part (curve a), no plateau appears; the local solidification rate at the bottom part is so fast that the recorder used in this experiment was not able to respond to it. However, the plateau appears at the upper part (curve b) due to the lower cooling (slope) rate as well as the longer local solidification time which can be measured. The cooling rates for both parts of the casting appear to stabilize after about 120 seconds. The cooling rate at the bottom part is around 20 °C/s, and 4 °C/s at the middle part, as shown in Fig. 3.1.10.

It was observed in the microstructure that a very fine structure was obtained near the chill surface and progressively coarser structures in the middle and the upper parts, as shown in Fig. 11.

Figure 11 shows that the graphite particles are present mainly in the upper part of the directionally solidified casting. This was probably due to the high flotation velocity of graphite particles resulting from the preexisting agglomeration of graphite particles. Generally, the distribution of graphite particles is expected to improve under the high cooling rates in thinner sections castings due to the reduction of flotation time of graphite particles. However, these observations show that a cooling rate of 20 °C/s (Fig. 3.1.10) may not be fast enough to significantly help in improving the distribution of graphite particles under present experimental conditions (where preexisting agglomerated particles do not deagglomerate in melt due to stirring). Thus to improve graphite distribution, the graphite particles must be greatly deagglomerated before their addition as well as during mixing, and the cooling rate should be enhanced. In addition to macrosegregation to the top part of the casting, the graphite particles are found to be present in the interdendrite regions as a result of pushing by the growing dendrite crystals. This is one of the problems to be solved to improve the distribution of graphite particles in the solidified matrix.

3.1.5. Microstructure Analysis of Fluidity Spirals

Metallographic samples from different locations of a fluidity spiral were examined under the optical microscope to observe the presence of graphite particles and the microstructure of the metal matrix. The dendrite arm spacing of samples taken from different locations of the castings fluidity spiral was also measured using the optical microstructure. An important feature of the copper alloy-graphite composite casting is the nature of graphite particle distribution throughout the casting. The results of the measurements of particle distribution showed that the volume fraction of particles in fluidity spiral varied with locations within the spiral.

Typical microstructures from two positions of fluidity spirals of copper alloy-graphite

composite are shown in Figs. 3.1.11 and 3.1.12. It is apparent from this figure that graphite particles originally of 5 μm size are present in large agglomerated clusters in the copper alloy castings; in addition, there is variation in the amount of graphite present in different parts of the spiral. The floatation velocity of these several hundred micrometer size clusters of graphite particles will be many times higher than that of 5-10 μm individual particles according to Stoke's law. This agglomeration apparently contributes to the macrosegregation of graphite in cylindrical and spiral castings. Thus, it is very necessary to deagglomerate graphite clusters before addition into the melt, and retain them as individual deagglomerated particles in the castings.

Micrographs indicate no significant difference in average secondary dendrite arm spacing of the matrix metal at the different locations on the same spiral (Figs. 3.1.11-3.1.12). The results of measurements of the dendrite arm spacing for yellow brass-1.5 wt% graphite composite are shown in Fig. 3.1.13.

3.1.6. Flotation

The floatation of graphite particles in copper matrix composite melt was studied on yellow brass-based matrix alloy with 0.8 wt% of graphite. This material was produced in an induction furnace. An intensive mixing of graphite powder was performed for deagglomeration of graphite particles before their introduction into the molten alloy.

Macroexamination of the longitudinal section of the zero holding time castings (Fig. 3.1.14) indicates no significant graphite floatation in the casting; microscopic examination showed a fairly uniform graphite distribution over the entire height of the casting; the presence of graphite apparently refined the grain size. Macroscopically this sample appears to be free of defects such as structural discontinuities. On the contrary, macroexamination of the second casting poured after ten

minutes holding shows the formation of two markedly different regions. The graphite-rich and graphite-free regions apparently formed due to floatation of graphite particles; these two regions (graphite free and graphite rich) are separated by an easily identifiable boundary because the grain size is finer in the graphite rich region.

Grain structures of the two regions of the casting made after holding are observed to be distinctively different. The as-cast grains in the graphite-rich zone appear much finer than in the graphite-free zone. It must be noted that there is some difference in the grain size of this casting section from bottom to top even though one does not macroscopically observe the formation of two clearly separated regions. The grain size decreases gradually from approximately 3 mm near the bottom part of casting to 0.5 mm in the layer at the upper part; suggesting some floatation of graphite. The results are indicative of the fact that graphite particles play a role in modifying structure and result in refinement of cast grain size in this copper alloy

3.1.7. CONCLUSIONS

1. Stirring of uncoated graphite alone in the Cu melt did not result in incorporation of any significant amounts of graphite in the melt or in the castings.
2. It is possible to disperse 1.0 to 2.0 wt% graphite in Cu alloy melts in castings by adding 0.5 to 1.0 wt% Ti to the melts. Over twenty heats of graphite containing copper were successfully made.
3. Percentage of recovery of graphite in the copper-graphite castings was observed to be higher with a higher wt% of Ti added to the copper melt.
4. An average of 80% incorporation of the added graphite could be achieved by a two-stage stirring technique and with the higher amount of Ti addition. The recoveries

of graphite using the two stage stirring technique are much higher than those obtained in single stage stirring.

5. Secondary dendrite arm spacing was not significantly affected due to graphite additions of up to 1.5 wt% indicating that the cooling rate of copper alloys was not significantly influenced by graphite additions.
6. A graphite-free zone is formed in some castings as a result of the floatation of graphite particles with increasing time of isothermal holding.
7. The presence of graphite particles results in a refinement of grain size in copper alloys.

3.2 Deagglomeration

3.2.1 Introduction

In the initial technology development, the distribution and recovery of graphite particles were improved using a suitable stirrer design, combined with a two-stage stirring technique. However, some large clusters of graphite particles still persisted. In as-received condition, finer graphite particles (-5 μm) are always present in clusters of particles. Even though graphite particles are heated to reduce their moisture content, the electrostatic forces acting between the fine particles do not fully dissipate even under intense shearing acting of melt stirring. The residual agglomerated clusters of graphite particles in the melt enhance their buoyancy effect and floatation takes place at a much faster rate causing an undesirable nonunfrom distribution.

3.2.2. Experiment

To obtain deagglomerated powder the graphite particles were mixed with aluminum powder in a glass container. This blended powder was used for the casting of yellow brass. To obtain deagglomerated powder, the sieve blending techniques was tried with graphite and a

powder resin, as shown in Figure 3.2.1. In addition, graphite particles were mixed with aluminum powder (Al:Gr = 1:2 by wt) in a glass container and then this mixture was used to make copper-graphite composites.

3.2.3. Results and Discussion

Figs. 3.2.1 through 3.2.4 show the mixed graphite-resin particle distribution following the preparation techniques shown in Figs. 3.2.1 a, b, and c, respectively. It may be noted that the addition of resin powder with graphite particle improves the distribution of graphite particles. A mixture of graphite particles and aluminum powder (10 μm) was obtained with intensive shaking in a glass container. This blended powder was used for the casting of yellow brass graphite composites with titanium as the wetting agent. Typical microstructure of the composite is shown in Figure 3.2.5. The figure shows that premixing with aluminum powder broke up the graphite agglomerates into individual graphite particles and they are distributed more uniformly in the matrix. Since for better properties uniform distribution is a must, the adoption of this method achieved this to a certain extent. The reduction in the cluster size also reduces the floatation velocity of the graphite particles and enhances uniform distribution in the melt. Microstructure observation shows that the above effect of aluminum powder remains effective though aluminum dissolves rapidly in copper alloy melt. Even after an hour at a temperature 950 °C, the size of agglomerate is about 50 μm as compared to the much larger agglomerates (800 μm) obtained using the graphite powder in the as received condition without mixing them with aluminum powder. According to the Stoke's law, the flotation velocity of the particle is a function of the square of the particle size. Therefore, an increase in the particle size by 10 times increases the floatation velocity 100 times. Because of the high alloying tendency of aluminum in copper

melt, the aluminum-graphite mixture added to copper melt has no tendency to form an agglomerate of its own.

3.2.4. Conclusion

To obtain deagglomerated powder, 10μm particle size aluminum powder was mixed intensively with graphite in 1:2 proportion. Typical microstructure of composite reveals that premixing with aluminum powder separates the graphite particles and they are distributed more uniformly in the matrix alloy. The procedure helps to obtain composites with more uniform distribution of the graphite phase and will significantly decrease the tendency for flotation.

3.3 Machinability

3.3.1. Introduction

Machinability tests were conducted on the copper graphite samples to study the effect of graphite on the machinability of castings. Some of the criteria normally used for rating machinability are volume rate, degree of tool wear, power requirements, machined chip length, machined surface roughness, temperature increment and vibration generation during machining. In our study, lathe and drilling tests were conducted for machinability evaluation of the composites.

3.3.2. Experiment

The samples for the machinability tests were made by preheating graphite particles to 200 °C in an oven before adding it to the melt at 1150 °C using the stir casting method. Both 60/40 brass and brass-1.5wt% graphite composites were cast into three inch long and one-inch diameter steel mold lathe-turning tests.

Lathe-turning tests: The samples were machined with a standard C3 carbide insert and cutting and feeding force data were obtained using three component dynamometer and labview software at Tufts University. All the samples were machines at 840 rpm at three different feed rates and depth of cuts. Chips were collected and inspected and photographed.

Drilling tests: To observe the effect of distribution of graphite particles on the machinability castings were made using two blade angles of 45 and 60 degrees. For drilling machinability three copper alloy samples were used: yellow brass, yellow brass containing 1.5wt% graphite and 2wt% Ti and C90300 –1.5wt% graphite and 2wt% Ti. Machinability tests were done on 25mm diameter cylindrical ingots along their length at equal spacing of 25mm starting from the bottom. A 5.8mm diameter, 60 degree included angle high speed drill was used at 440rpm under a constant 5kg force. The depth of the drill corresponded to the diameter of the cylindrical ingot. Chips from these tests were collected and analyzed for total number and total weight.

3.3.3. Result and Discussion

Figures 3.3.1 and 3.3.2 show the machinability force data for 1inch and 3-inch diameter brass and brass –graphite composite castings. These figures show that cutting forces increases with increase in feed rate and depth of cut, and the cutting force for brass-graphite composite is lower than that of brass and as the depth of cut and the feed rates increase the feed force also increases. These machinability tests show that the presence of graphite particles in copper alloy matrix significantly improves machinability.

Drilling tests: The tests showed that the chips from the composite were significantly smaller that those of the monolithic alloy yellow brass and the size of the chips is the reciprocal to the number of chips per gram. The chip size varied from the bottom to the top of the castings.

The size of the chip was smaller at the top than the bottom, which could be related to the higher content of graphite at the top, as graphite acts as a chip breaker. The chips from C90300 alloy composite gave a fairly uniform chip size throughout locations. The chip size was significantly smaller than from yellow brass at all locations. Comparison of the effect of the blade angle on the distribution of graphite in the castings showed that the 60-degree blade produced a good graphite distribution form the bottom to the top of the casting.

3.3.4. Conclusion

1. The machinability tests showed that dispersed graphite particles in the matrix of copper alloys improve machinability and decrease both the cutting and feed forces significantly. In addition, at higher feed rates and depth of cut, graphite particles reduce the cutting and feed forces to a great extent. Therefore, it can be expected that the graphite particles being soft, the wear rate of the tool will be reduced.
2. The drilling test showed that the presence of graphite particles reduces the chip size.

3.4 Centrifugally Cast Copper Alloy Graphite Composites

3.4.1. Introduction

Stir casting techniques involving mixing of particles in the melts prior to solidification has been widely used for solidification synthesis of cast metal matrix composites due to its simplicity. This technique has several problems ; (i) frequently observed poor wetting of ceramic particles by the melt, requiring the external forces to introduce the particles into the melt, (ii) floatation or sedimentation of particles in the melt due to the density difference between the particle and the melt (iii) the segregation of the particles in the last freezing interdendrite regions

due to the rejection of the particles by the solidifying interface. However, unlike the gravity casting, centrifugal casting technique of melts containing suspended particles leads to segregation of particles in the inner periphery or the outer periphery of the centrifugal casting, depending on the density difference between the particle and the melt. Centrifugal casting provides selective reinforcement as a result of segregation of the particles to the inner or outer periphery of centrifugal casting. It therefore presents an ideal technique to produce components like cylindrical bearings where tribological surfaces are required only at the inner surfaces of cylinders. In fact the concentration of particles to the inner periphery for bearing type applications leads to other benefits including reduced requirements of the dispersoid compared to the castings where the particles are uniformly distributed. In addition the outer periphery of casting remains free from dispersoids leaving their properties intact.

3.4.2. Experimental Procedure

C90300 copper alloy was melted in a graphite crucible using an induction furnace. 5 μm graphite particles and 1.5 wt.% Ti (used as wetting agent) were mixed into the copper alloy to synthesize copper alloy melt containing 7 vol.% and 13 vol.% graphite particles. The mold inserted in the horizontal centrifugal casting machine was preheated at 200 °C. At the melt temperature of 1050 °C, the molten copper alloy was poured into the horizontal centrifugal casting machine to cast cylinders of copper alloy originally containing an average of 7 vol.% (2 wt.%) and 13 vol.% (3.6 wt.%) graphite particles. The copper alloy containing 7 vol.% of graphite particles represents the melts in which 7 vol.% graphite particles were added and also copper alloy containing 13 vol.% graphite particles represents the melts in which 13 vol.% of graphite particles was added. The outer diameter of the cylindrical castings was 9.5 cm, the wall

thickness was 1.5 cm and the speeds of rotation were 800 rpm and 1900 rpm. The length of the casting was 13 cm.

3.4.3 Results and Discussions

Graphite particle in the copper melt under centrifugal forces move to the inner periphery due to its lower density than that of the copper melt, leading to the formation of the graphite rich zone near the inner periphery of the centrifugal casting. Figure. 3.4.1 shows the microstructure near the outer and inner periphery of centrifugally cast copper alloy containing 7 vol.% graphite particles, cast at 800 rpm, indicating that graphite particles are segregated near the inner periphery of the centrifugal casting due to the lower density of graphite particle than that of the copper melt; in addition the graphite particles appears to be segregated in the interdendritic region due to the pushing of the graphite particle by the solid liquid interface. The particle pushing phenomena has been explained according to the critical interface velocity, below which the particles are pushed by the interface, and above which they are engulfed by the interface. In view of this, it can be inferred from this figure that the graphite particles are pushed by the solid liquid interface due to its lower velocity than the critical interface velocity. The microstructure also shows the presence of porosity in addition to the graphite particles.

The result of the chemical analysis of two copper alloy containing graphite particles from the inner periphery to the boundary near the graphite free zone shows that the graphite particles has concentrated near the inner periphery to an average of 16.3 vol.% (4.54 wt.%) graphite particles for the alloy containing 13 vol% (3.6 wt.%) graphite particles. For the alloy containing 7 vol.% (2 wt.%) graphite particles, the graphite concentration are an average of 13 vol.% (3.6 wt%) graphite particles near the inner periphery. It can be noted that as the volume fraction of the

graphite particles in the starting melt increases, the volume percent of the graphite particles segregated near the inner periphery increases.

During the synthesis of composites, all the particles added to the melt are not recovered in the castings. During the mixing or pouring the molten copper melt containing graphite particles into the mold, the particles are lost, leading to a decrease in the recovery of the particles. In this study, Ti is used as a wetting agent to improve the recovery of graphite particles, because TiC formed on the surface of the graphite particle is wettable by liquid copper. The recovery of the graphite particles in the centrifugal casting is calculated by dividing the graphite volume fraction in the graphite rich zone which is converted to that at the initial surface area of the centrifugal casting by the originally added graphite particles into the copper melt :

$$\text{Recovery} = \frac{\varepsilon_p'}{\varepsilon_p} = \left(\frac{\left(\frac{r_t}{r_0}\right)^2 - x^2}{1 - x^2} \right)$$

where ε_p is the volume fraction of the particle added initially into the melt and r_t is the thickness of the particle rich zone. ε_p' is estimated by measuring the average volume fraction of the particle at the particle rich zone. As a result, the recovery of the graphite particles is 97 % and 95 %, for the copper alloys originally 7 vol.% and 13 vol.% graphite particle, cast at 800 rpm, respectively.

3.4.4 Conclusions

1. Centrifugal casting (O.D 9.5 cm x I.D 8 cm) of copper alloy originally containing 7 vol.%

and 13 vol.% graphite particle were cast at 800 rpm and 1900 rpm. Microstructural observations and chemical analysis show that the content of graphite particles segregated and the amount of the porosity is higher near the inner periphery compared to that near the graphite free zone. Also, microstructure in the graphite rich and free zones indicates that the graphite particles are pushed in the interdendrite regions by the growing α copper dendrite.

2. The recoveries of graphite particles in copper alloys, calculated based on the content of graphite particles in the graphite rich zone, was found to be around 99% and 95%, for cases when 7 vol.% and 13 vol.% graphite particles were originally added to the melt, respectively, before centrifugal casting.

3.5 Tribological Properties of Centrifugally Cast Lead Free Copper Alloy Against Cast Iron and SAE 1045 Steel

3.5.1 Introduction

In this study, relative tribological properties of the centrifugal cast C90300 originally containing 13vol% graphite particles, have been characterized, including friction coefficient, wear rate, variation of weight of pin and counterface, temperature rise of the counterface. These test were conducted against cast iron and steel counterfaces and a comparison was made between the tribological properties of the graphite rich and graphite free region, base alloy and the C90300-13 vol% graphite composite and C90300-13 vol% graphite composite and leaded copper alloy at different conditions of applied load and speed. During sliding, several phases from the pin are transferred to the counterface or vice versa, and the shape of debris formed will depend on the presence of reinforcements in the matrix. Therefore, the transfer of the phases from the pin to the counterface, or vise versa, was measured.

3.5.2. Experiment

Pins of copper alloy C90300 containing graphite particles were machined to 6mm diameter and 15 mm length and tested under dry condition at four different loads ranging from (i) 44.5 to 267N for 5 minutes against a cast iron counterface (78HRF), (ii) 44 to 176N for 30 minutes against a SAE 1045 steel (28-32HRC) counterface at a speed of 1m/s and (iii) C90300 containing 13 vol% graphite particles and leaded copper alloy (22% Pb) at load of 57N and speed of 0.625m/s and 26.2N at a speed of 1.25 m/s against a SAE 1045 steel (58-60HRC) counterface for 60 minutes. Before each test, the counterface was cleaned with acetone to remove any chemical elements. Temperature at 2mm below the tribosurface was measured using a chromel-alumel thermocouple and torque value was recorded. The temperature was recorded to an accuracy of 0.1°C and the torque to 0.1lb-in. From the torque data recorded, the friction coefficient was calculated using the following equation.

$$f = \frac{T}{(L^* R)}$$

f is the friction coefficient

T is the torque in lb-inch

L is the applied load in lb

R is the radius of the wear track in inch.

After the tests the pin and disk were cleaned again and their weights taken. The results of these test data were analyzed for:

Coefficient of friction

Change in weight of pin and disk

Temperature rise

The microstructure and scanning electron microscopy of the pin and the disk before and after the test were also taken. The wear debris generated during the test was collected and EDX analysis of the wear debris, pin and disk was done to determine the change in the surface composition brought about by the running of the pin against the disk.

3.5.3. Results and Discussion

The values of the friction coefficient obtained under different condition are given in Tables 3.5.1 to 3.5.3. In case of the friction coefficient of the graphite rich zone and the graphite free zone, the friction coefficient of the graphite rich zone increases with increase in load upto 133.5 and then slightly decreases at 267N. The friction coefficient of the graphite rich zone was found to be lower than that for the graphite free zone at all the applied loads. As seen from table 3.5.2 and 3.5.3, the friction coefficient for the C90300-13 vol% graphite pins was lower than or equal to that of the base alloy C90300 and leaded copper alloy at all applied loads and speeds. The variation in the friction coefficient of the C90300-13 vol % graphite pin with applied load may be related to the gross deformation of the pin and the disk and their mutual adhesion, transfer and back transfer of layers of the material and a change in the mechanism of tribo deformation and the nature of the tribo surface with applied load. As the applied load increases, the graphite particles in the matrix can get squeezed out and be smeared on the surface of the pin due to the tangential force. The graphite is thus able to form a film, which prevents direct metal to metal contact and reduces friction. Thus graphite seems to perform similar to lead in leaded copper alloys. This can be further clarified by the friction coefficient value obtained for the copper graphite composite and the leaded copper alloy as given in Table 3.5.3. For efficient

lubrication, the film formed must stay long enough on the surface, which depends on the deformation characteristics of the matrix and also on the size of the graphite particles.

The weight loss data for the three different sets of test conditions is shown in Figures 3.5.1 to 3.5.3. The weight loss of the copper graphite pin was found to be lower than that of the base alloy as well as the leaded copper alloy at all the applied load. All the figures show that the weight loss of the pin increases with increase in the applied load. From figure it is seen that the weight loss of the base alloy pin increases from 0.00437g at 44N to 0.01367g at 176N whereas the weight loss of the copper alloy pin increases from 0.00283g to 0.0092 g in the same load range. It can be noted from the results of the weight loss of the C90300-13 vol% graphite composite pins was much lower than that of leaded bronze pins. The presence of lead in bronze does not seem to impart good wear resistance as graphite in C90300.

The temperature rise at 2mm below the counterface plotted for all the three conditions is shown in Figures 3.5.4 to 3.5.6 at different applied loads. Except for the leaded bronze pins the temperature rise for the composite pins was always lower than the pin from the graphite free region as well as the base alloy at all applied loads. The above behavior may possibly be related to the presence of graphite in the matrix, which reduces the heat generated due to low friction.

EDX analysis of the surface of the pin from the base alloy (Figure 3.5.7.a) shows a significant peak of iron which is an indication of metal transfer from the disk, where as the iron peak is very small in case of copper graphite pin (Figure 3.5.7.b) run under similar conditions. This shows that there has been a reduction in metal to metal contact in case of copper graphite pins, which could have been due to the presence of graphite in the composite pin. Thus graphite, by forming a film on the surface of the pin, not only reduces the friction coefficient and the temperature rise but also reduces the metal transfer from the disk to the pin. SEM picture of the

surface of the pin taken from the base alloy C90300 (Figure 3.5.8.a) shows greater damage than that for the pin from the graphite rich region of the centrifugally cast C90300 originally containing 13 vol% graphite particles (Figure 3.5.8.b) when tested at the applied load of 44N against 1045 steel counterface. EDX analysis of the wear debris generated, when the base alloy pin (Figure 3.5.9a) and centrifugally cast C90300 originally containing 13 vol% graphite (Figure 3.5.9b) were run against a 1045 steel counterface at applied load of 176N, shows significant peak for iron. Similar data was found when the base alloy pin was analyzed. The greater amount of iron found in the wear debris in case base alloy pin indicates greater loss of material from the counterface as compared to tests run using centrifugally cast C90300 originally containing 13 vol% graphite particles. From the tests conducted so far we can infer that the centrifugally cast copper alloy containing graphite particles perform better than the base alloy C90300 and leaded bronze alloy from the point of view of bearing application.

3.5.4. Conclusions

The pin on disk test of the centrifugally cast copper alloy originally containing 13vol% graphite particles, showed that the presence of graphite particles near the inner periphery improves tribological properties. The friction coefficient and weight loss of the pin of pin from the graphite rich region was lower than that of the pin from the graphite free region, and the base alloy C90300. While the friction coefficient of the pin from the graphite rich region was similar to that of leaded (22% Pb) copper alloy, the weight loss of the pin from the graphite rich region was much lower than the weight loss of the leaded (22% Pb) copper alloy pin.

The temperature of the counterface running against the pin from the graphite rich region, graphite free region, and base alloy C90300 increased with increase in applied load. The

temperature of the counterface running against the pin from the graphite rich region was lower than that of the pin from the graphite free region, base alloy C90300. However the temperature of the counterface run against the leaded copper alloy was lower than that of the pin from the graphite rich region.

Table 3.5.1. Steady state friction coefficient for graphite free and graphite rich zones of centrifugally cast copper alloy C90300 originally containing 13 vol% graphite particles.

Material	44.5N	89N	133.5N	267N
Graphite free region	0.52	0.65	0.69	0.75
Graphite rich region	0.02	0.45	0.49	0.4

Table 3.5.2. Steady state friction coefficient for base alloy C90300 and centrifugally cast copper alloy C90300 originally containing 13 vol% graphite particles.

Material	44N	88N	176N
C90300	0.47	0.4	0.3
C90300-13% graphite	0.35	0.32	0.26

Table 3.5.3. Steady state friction coefficient for Leaded (22%) copper alloy and centrifugally cast copper alloy C90300 originally containing 13 vol% graphite particles.

Material	26.2N at 1.25m/s	57N at 0.627m/s
Leaded copper alloy	0.38	0.24
C90300-13% graphite	0.38	0.24

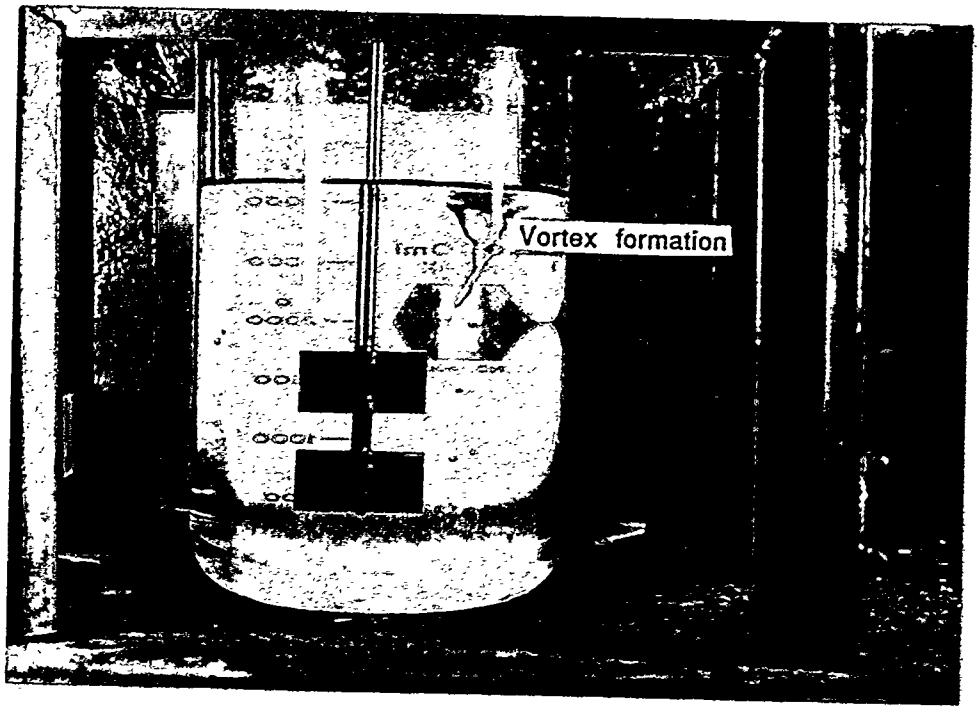

(a) 655 rpm

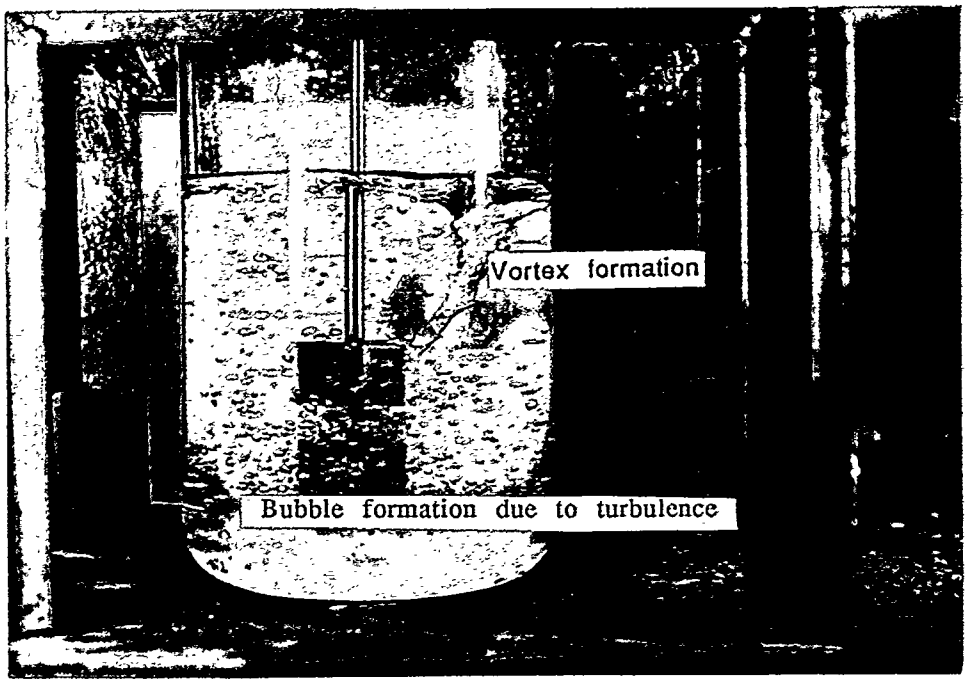

(b) 750 rpm

Fig. 3.1.1 Bubble and vortex formation when 90 degree blades are used to stir water different speeds

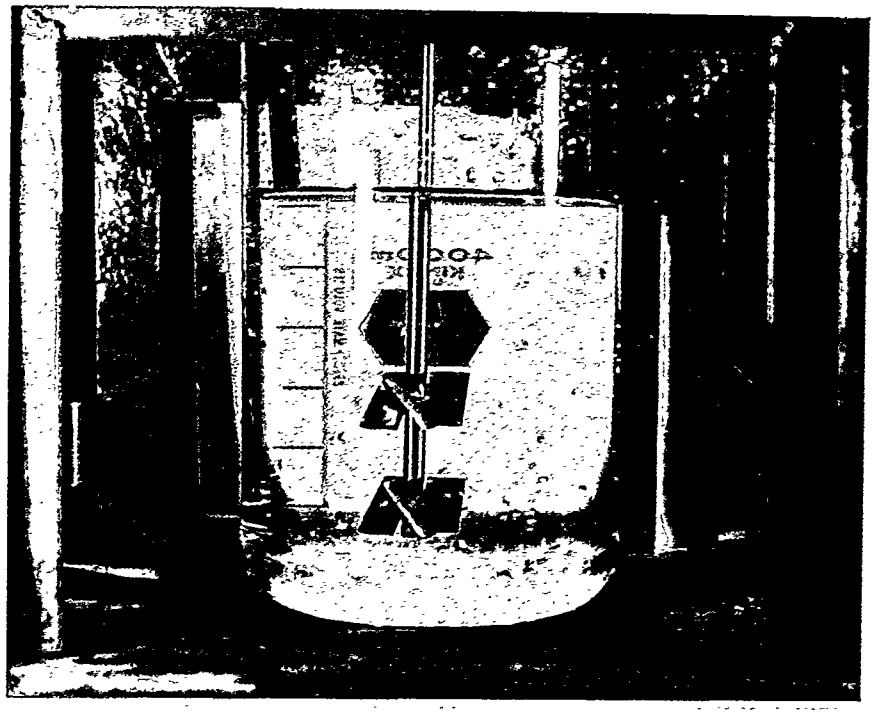

(a) 1000 rpm

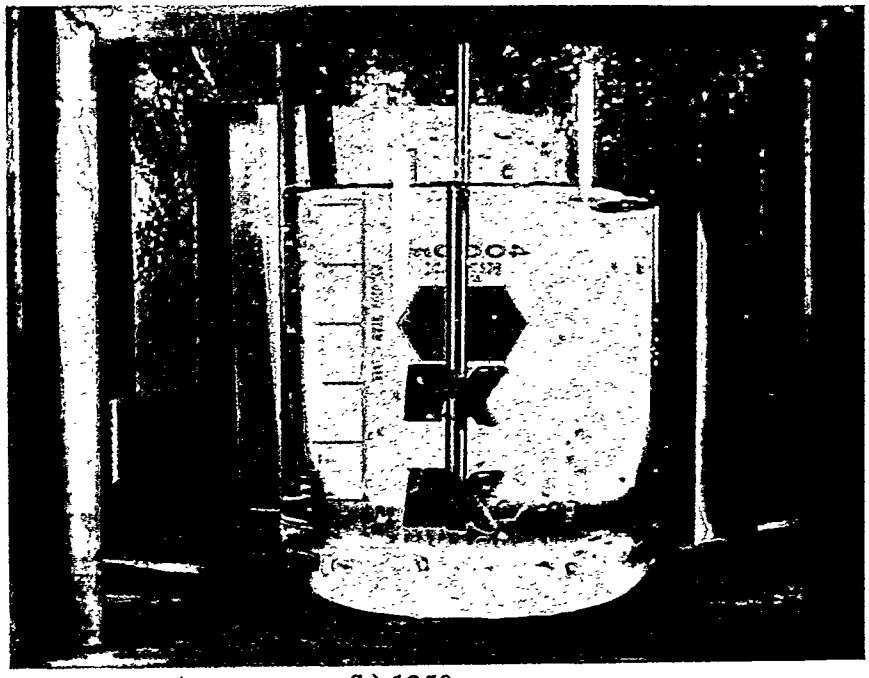

(b) 1250 rpm

Fig. 3.1.2 Bubble and vortex formation when 60 degree blades are used to stir water at different speeds

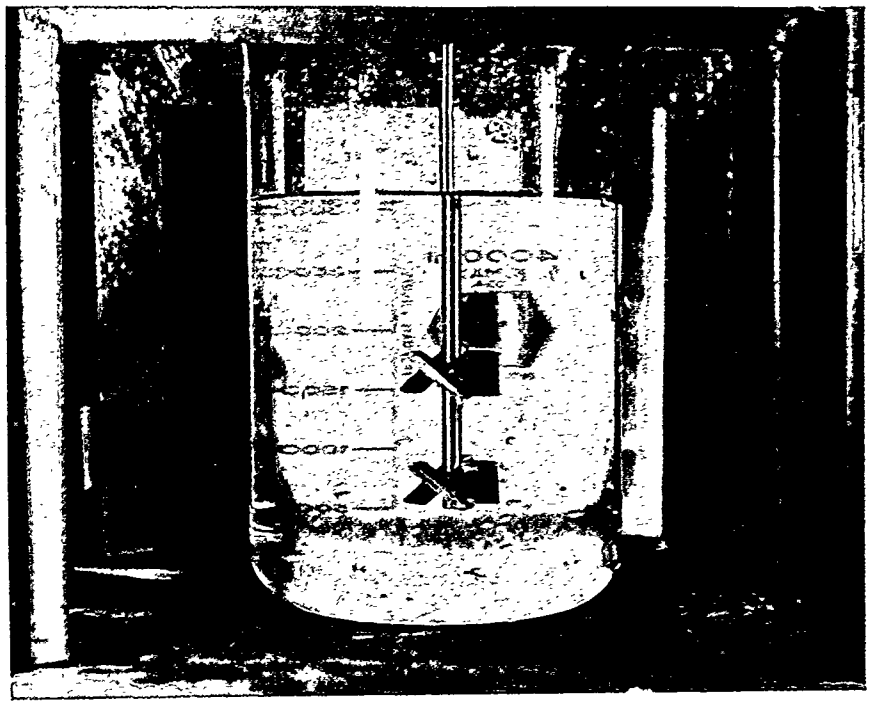

(a) 625 rpm

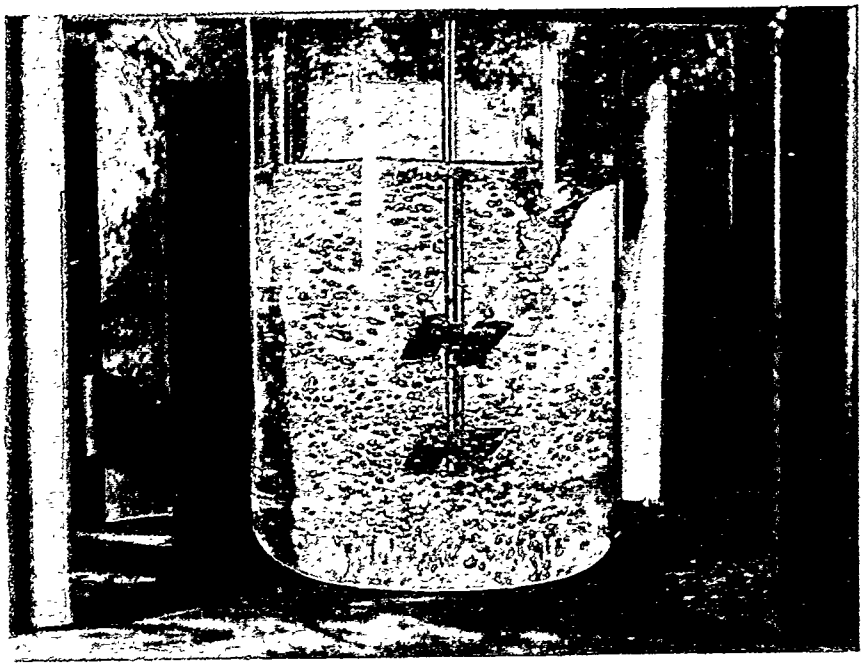

(b) 1000 rpm

Fig. 3.1.3 Bubble and vortex formation when 45 degree blades are used to stir water at different speeds

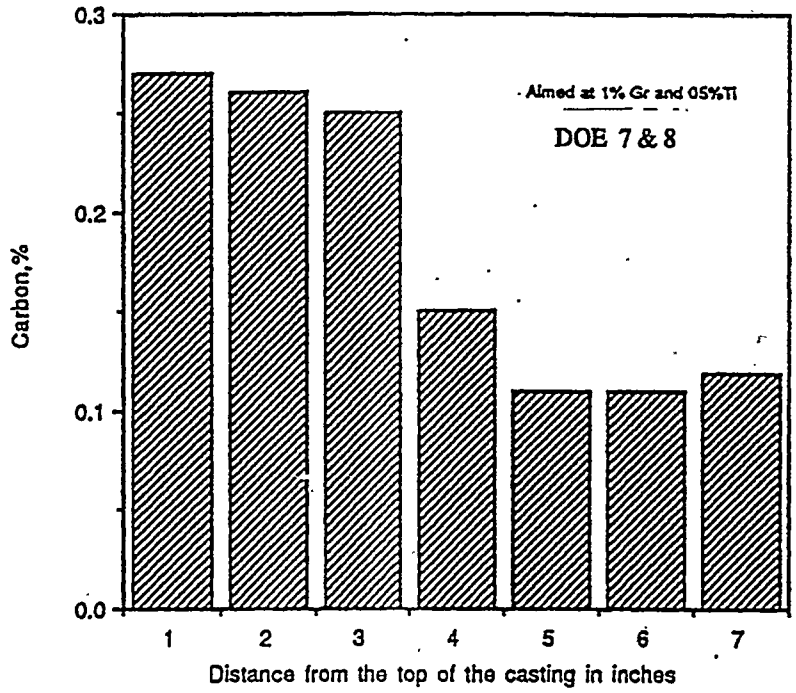

Fig. 3.1.4 Chemical analysis for carbon along the length of 1 inch diameter rod (DOE 7 and 8).

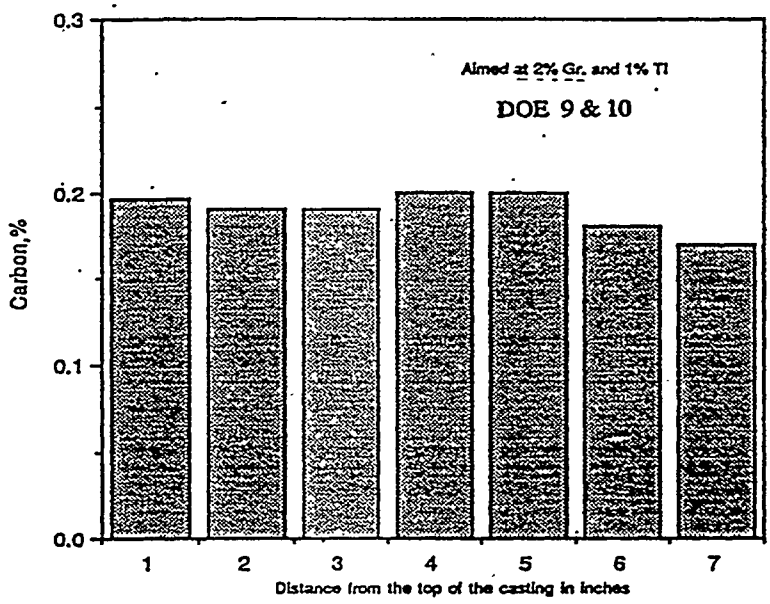

Fig. 3.1.5 Chemical analysis for carbon along the length of 1 inch diameter rod (DOE 9 and 10).

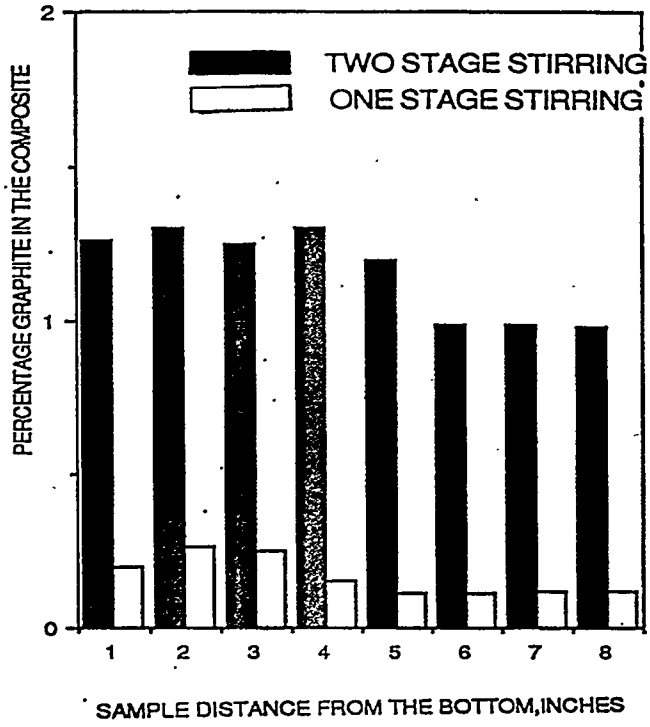

Fig. 3.1.6 Variation in graphite percentage in the composite castings when stirred in one-stage and in two-stages

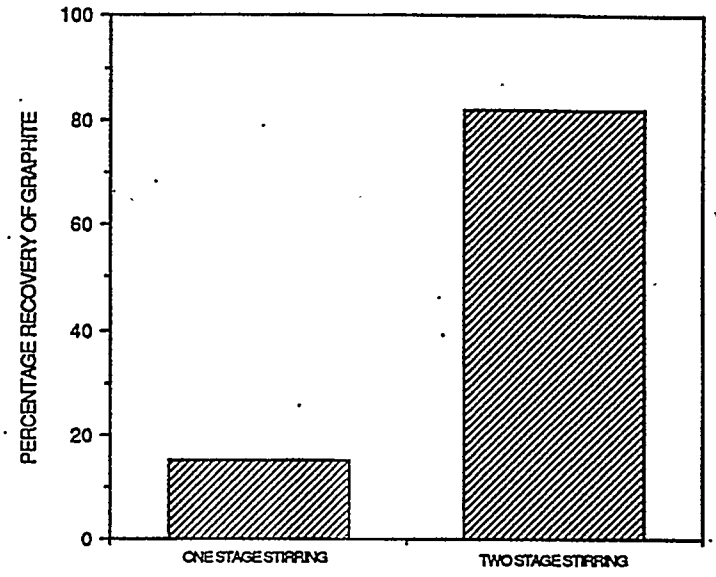

Fig. 3.1.7 Improvement in graphite recovery due to two stage stirring: this may reduce titanium and graphite requirement

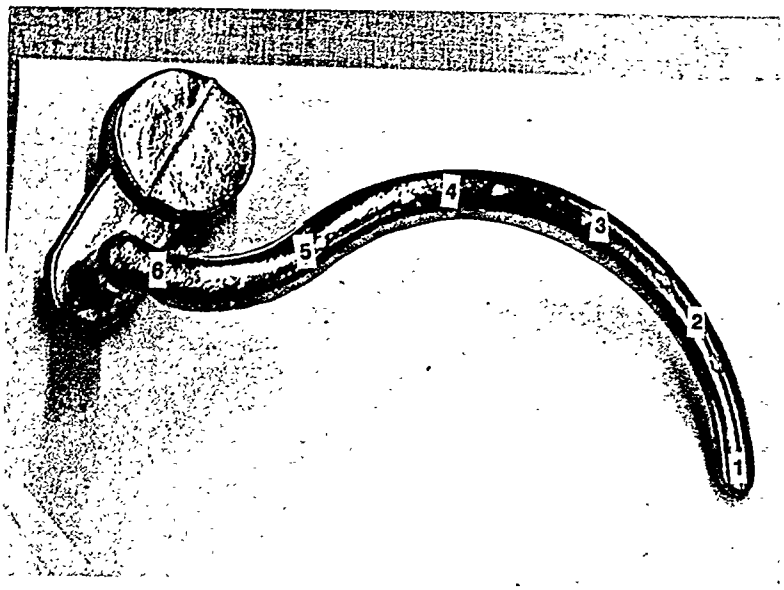

Fig. 3.1.8 Numbered locations from which samples were taken for metallographic examination.

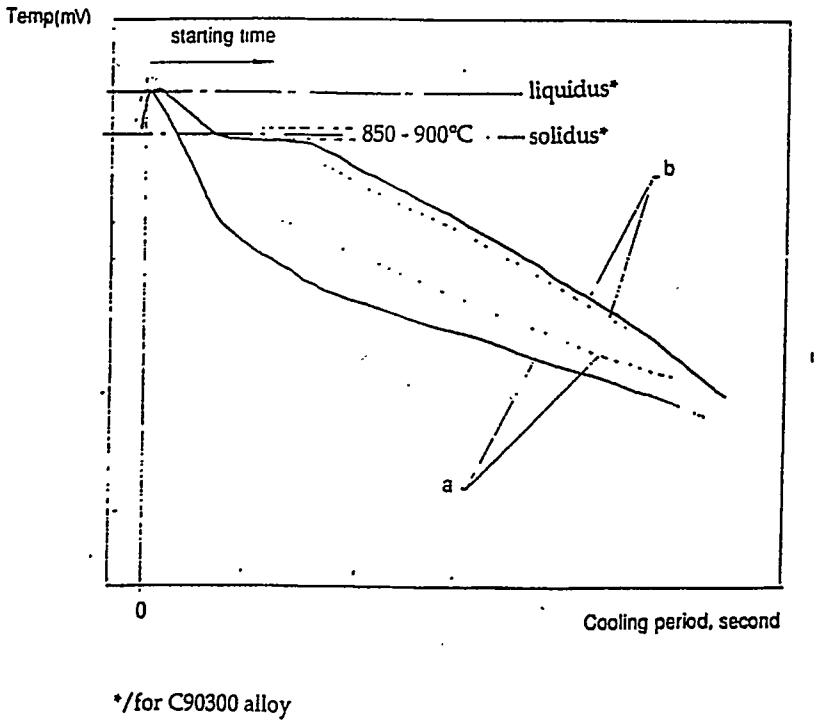

*/for C90300 alloy

Fig. 3.1.9. Typical cooling curves of C90300 of copper alloy-graphite composite in directional solidification experiments. The thermocouples are located near the bottom (a), and central and upper (b) parts of the mold.

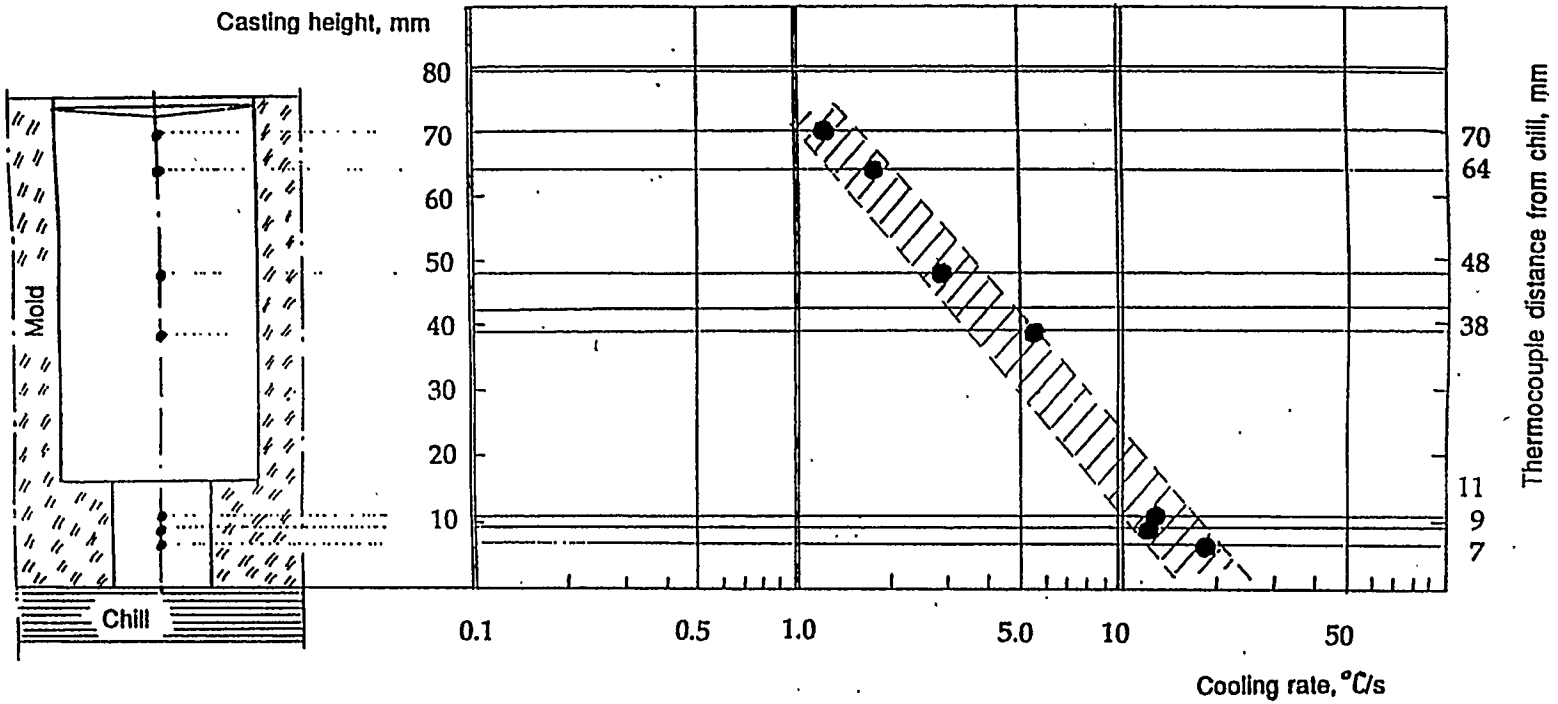

Fig. 3.1.10. Variation of cooling rate with casting height; location of thermocouples are shown at left.

(a) position #1, end (see Fig. 3.1.8)

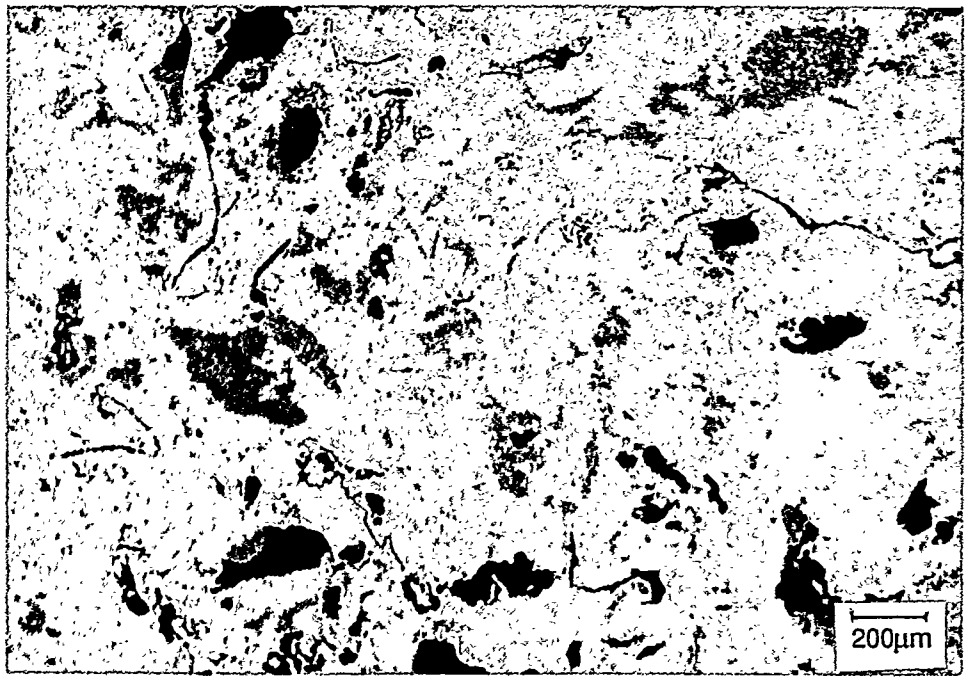

(b) position #6, entrance (see Fig. 3.1.8)

Fig. 3.1.11. Photomicrographs of fluidity spiral of yellow brass-1.5 wt% graphite - 1 wt % Ti composite, showing distribution of graphite.

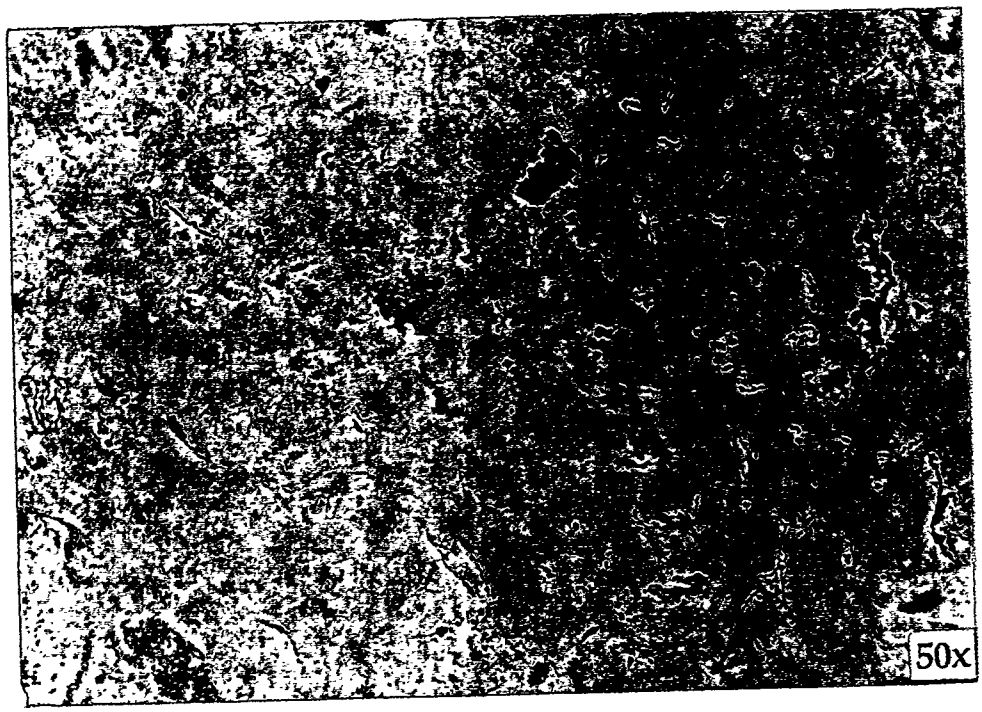

(a) position #3

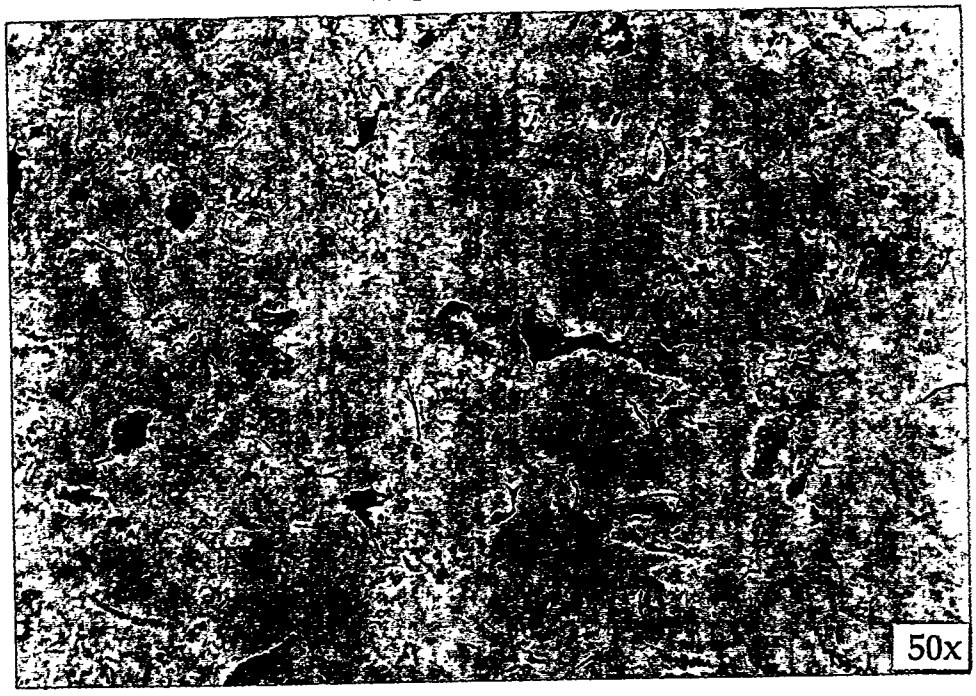

(b) position #4

Fig. 3.1.12. Photomicrographs of fluidity spiral of yellow brass-1.5 wt% graphite - 1 wt% Ti composite, showing distribution of graphite.

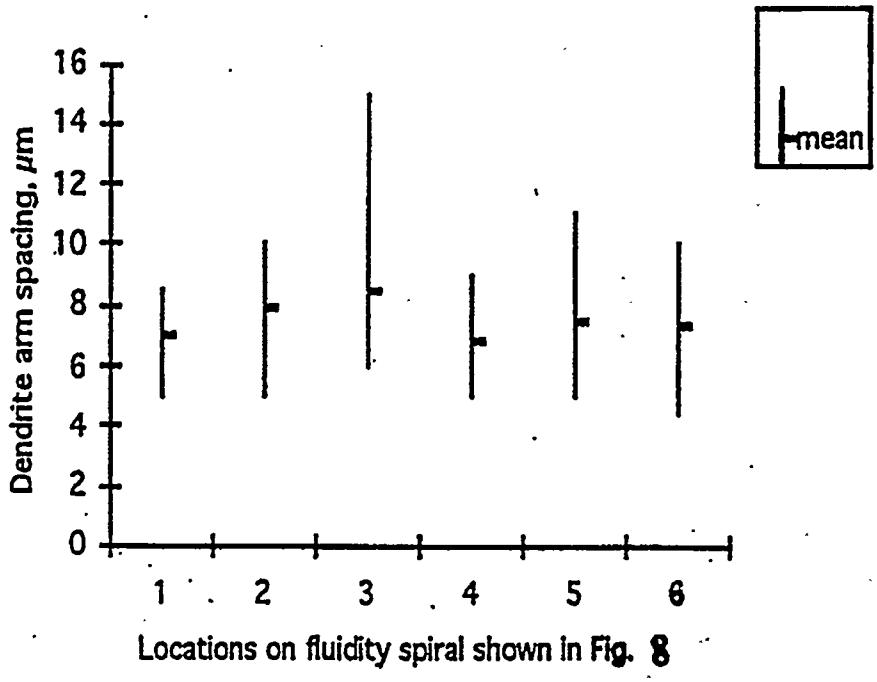

Fig. 3.1.13. Variation of dendrite arm spacing of yellow brass matrix at different locations of casting fluidity spiral copper-graphite alloys.

Fig. 3.1.14. Macrograph at the copper alloy-graphite casting poured into mold without any isothermal holding at 1000 °C (i.e., zero holding time).

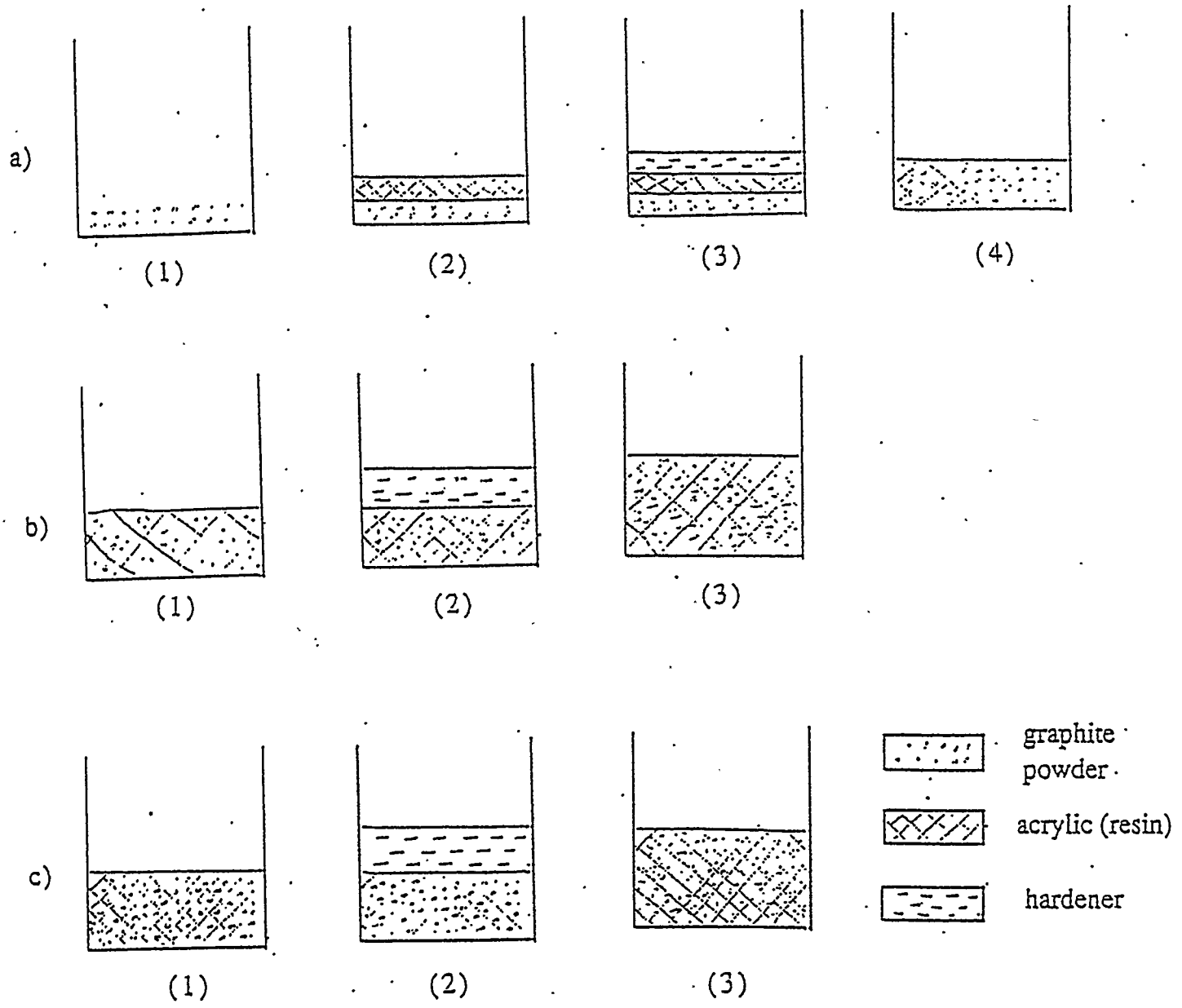

Fig. 3.2.1. Schematic distribution of different techniques for preparing graphite powder samples for microstructural observation:
(a) the layer by layer technique, (b) sample mixing by blending of two powders, and (c) mixing by intensive shaking of two powders

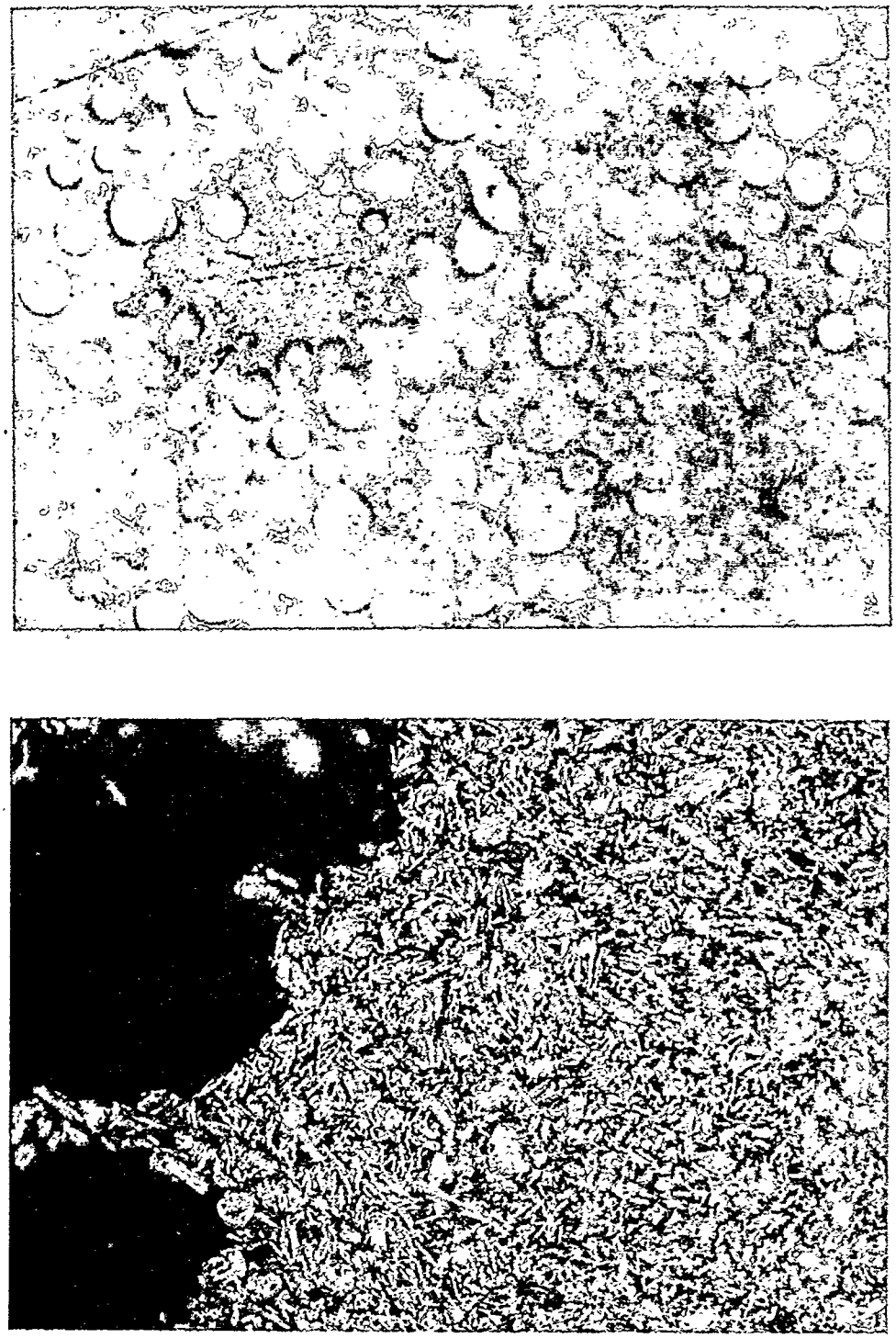

Fig. 3.2.2. Microstructure of a mixture of graphite and resin powder obtained by mechanical blending of two powders. (a) x50 and (b) x500.

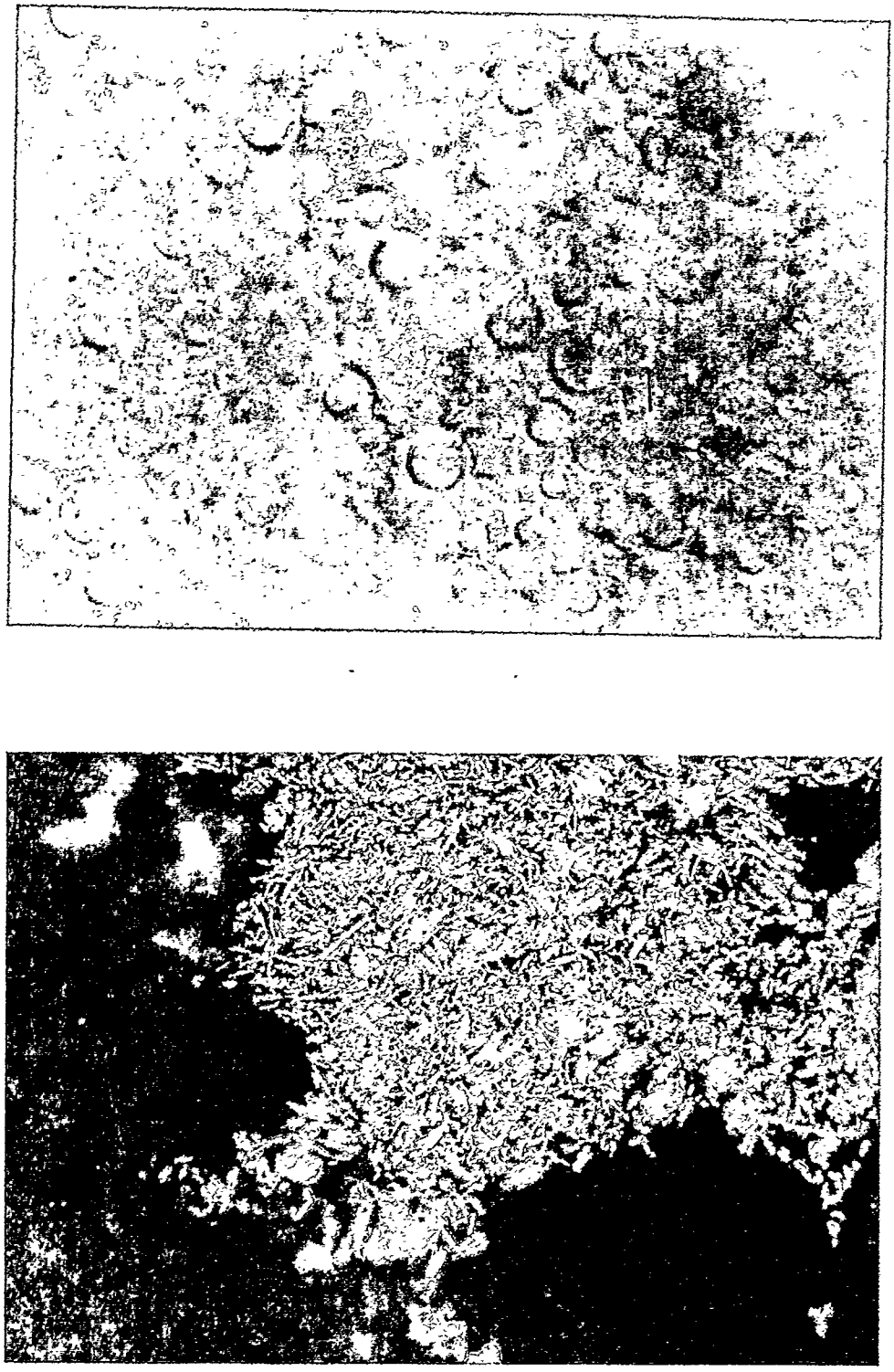

Fig. 3.2.3. Microstructure of a mixture of graphite and resin powder obtained by blending using a layer by layer technique. (a) x50 and (b) x500.

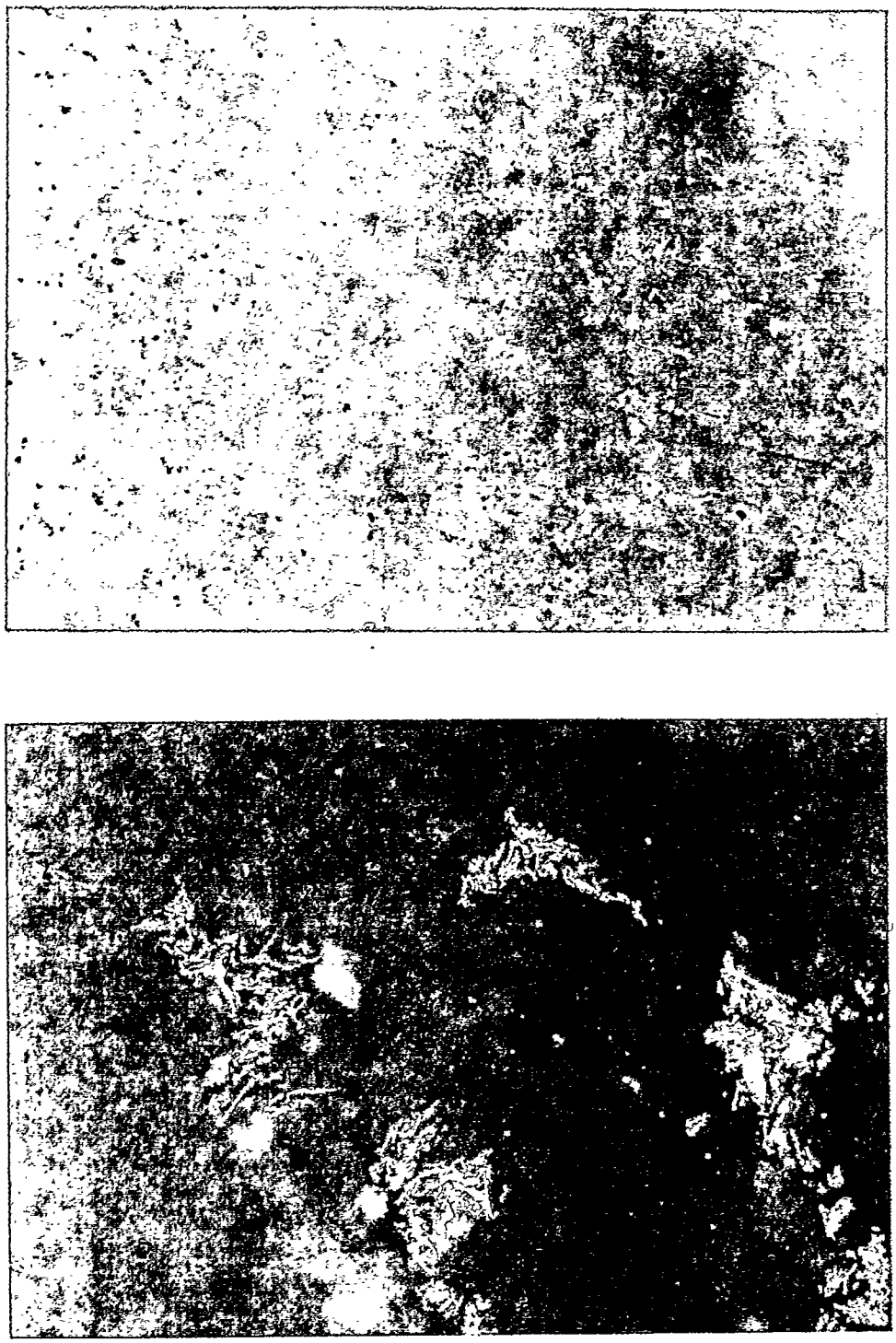

Fig. 3.2.4. Microstructure of a mixture of graphite and resin powder obtained by intensive shaking of two powders. (a) x50 and (b) x500.

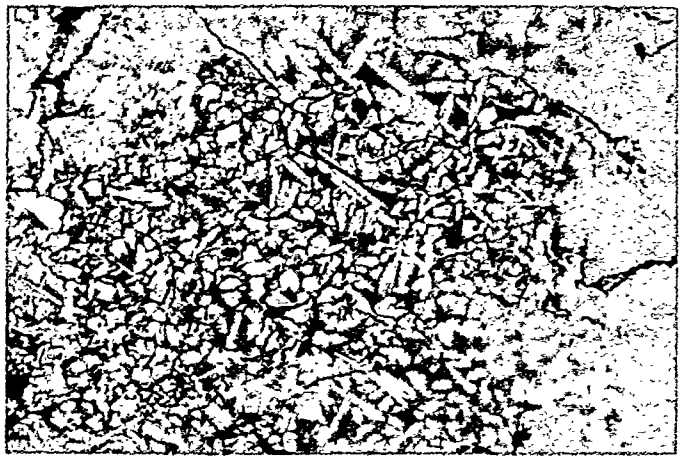

(a)

(b)

Figure 3.2.5. Microstructure of a yellow brass –graphite composite casting obtained using a mixture of graphite and aluminum. a) 200X, b) 500X.

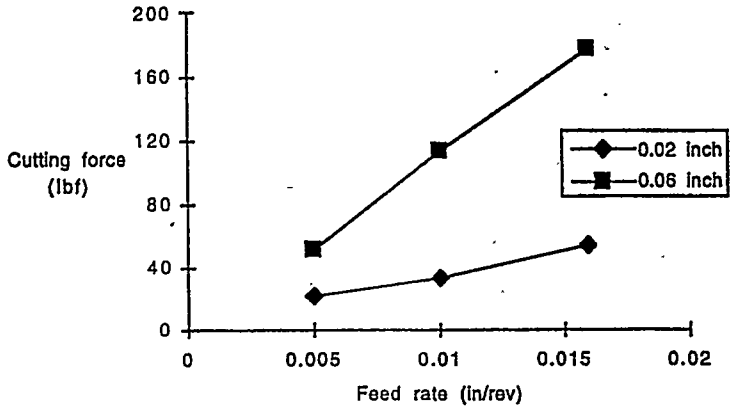

(a)

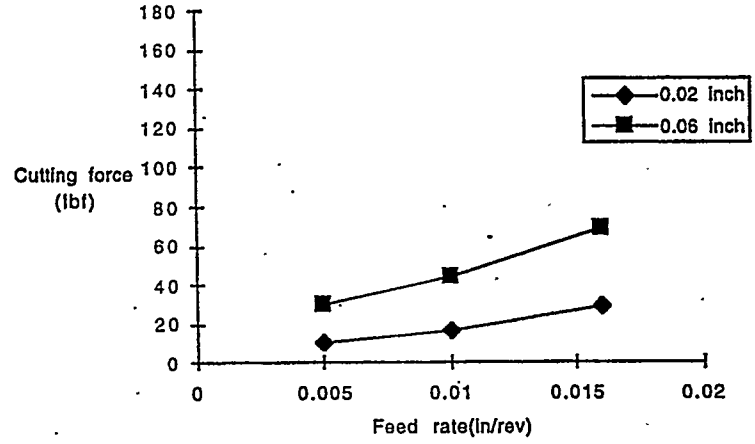

(b)

Figure 3.3.1. Cutting force as a function of feed rate and depth of cut in lathe turning of monolithic brass and brass-graphite composite of one inch diameter at 660sfpm.
(a) monolithic brass, (b) brass-graphite.

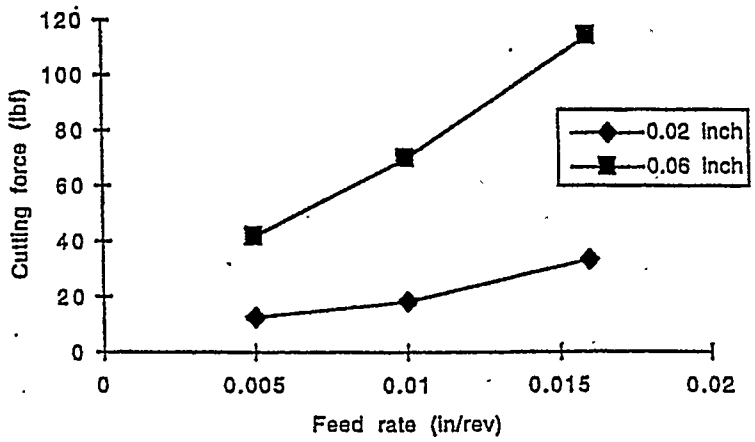

(a)

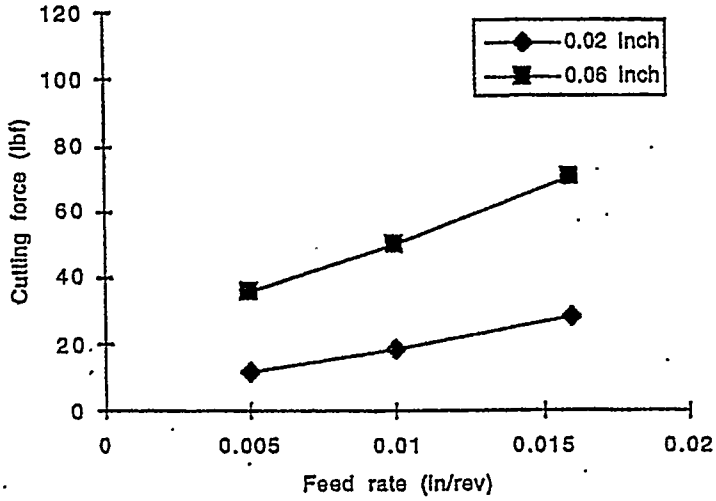

(b)

Figure 3.3.2. Cutting force as a function of feed rate and depth of cut in lathe turning of monolithic brass and brass-graphite composite of three-inch diameter at 660sfpm.
(a) monolithic brass, (b) brass-graphite.

Centrifugally Cast Copper Graphite Composite

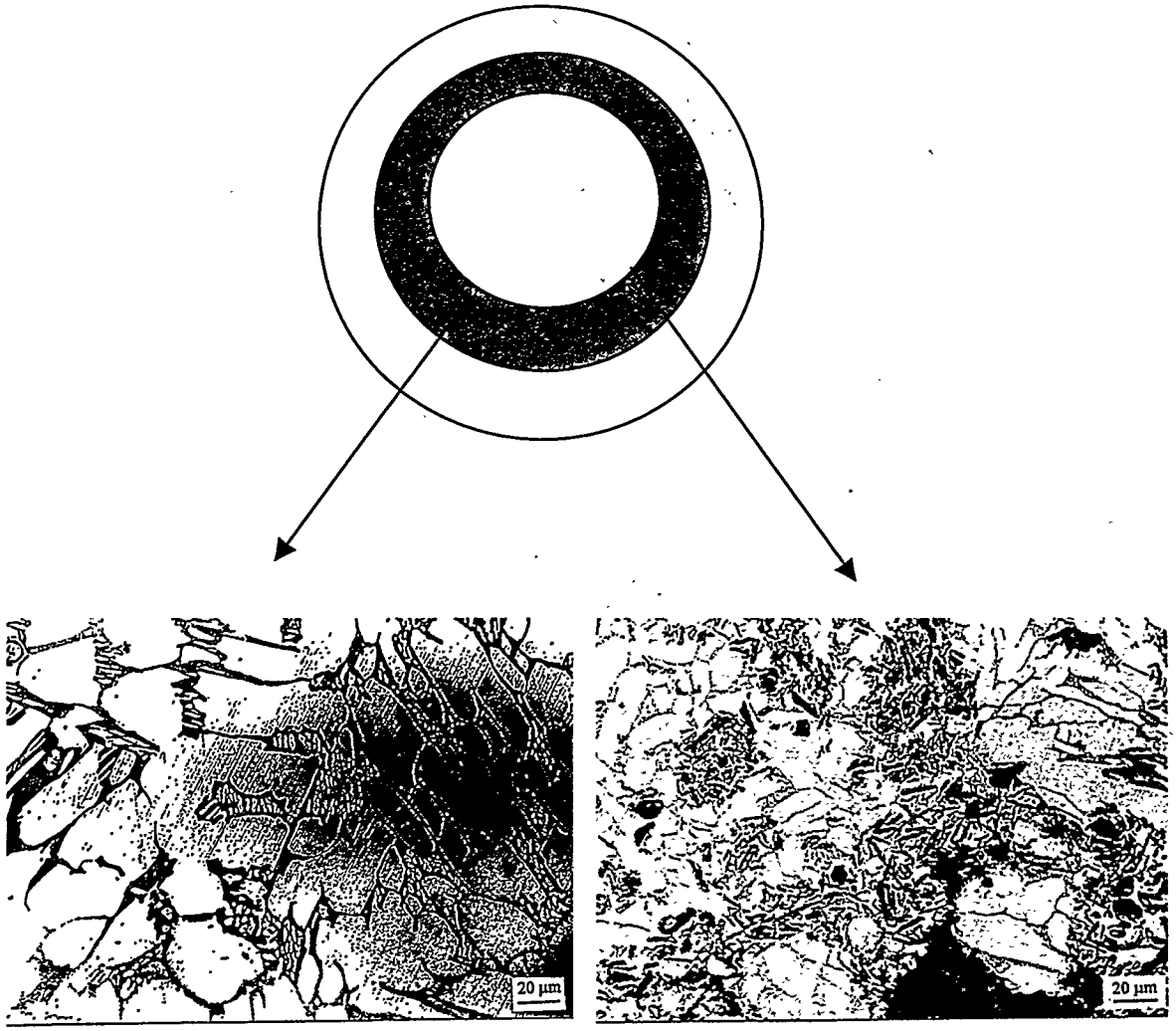

(a) Graphite-free zone

(b) Graphite-rich zone

Fig.3.4. 1. Microstructure near outer and inner periphery of centrifugally cast copper alloy containing 7 vol% graphite particles, cast at 800 rpm

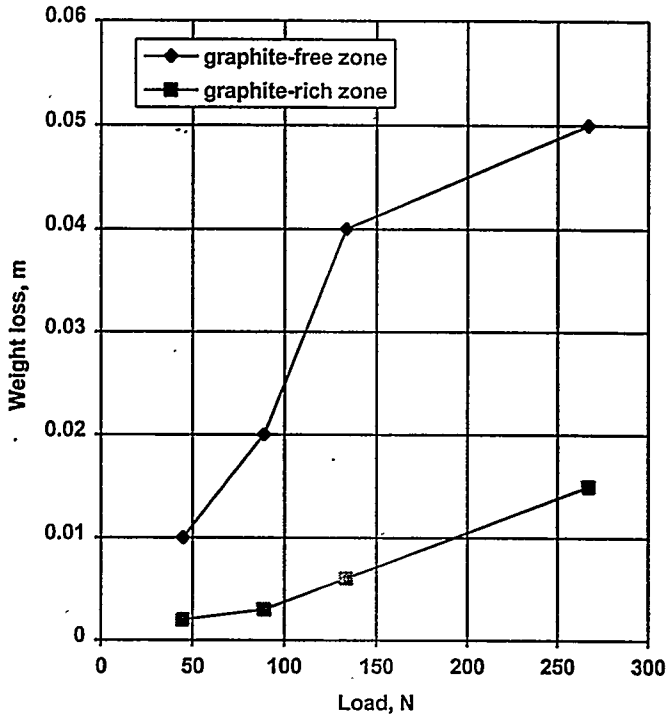

Fig.3.5. 1. Variation of weight loss of the pin from the graphite-rich and the graphite-free zones of C90300-graphite alloys with applied load after running against cast iron for 5 minutes and at a speed of 1m/s.

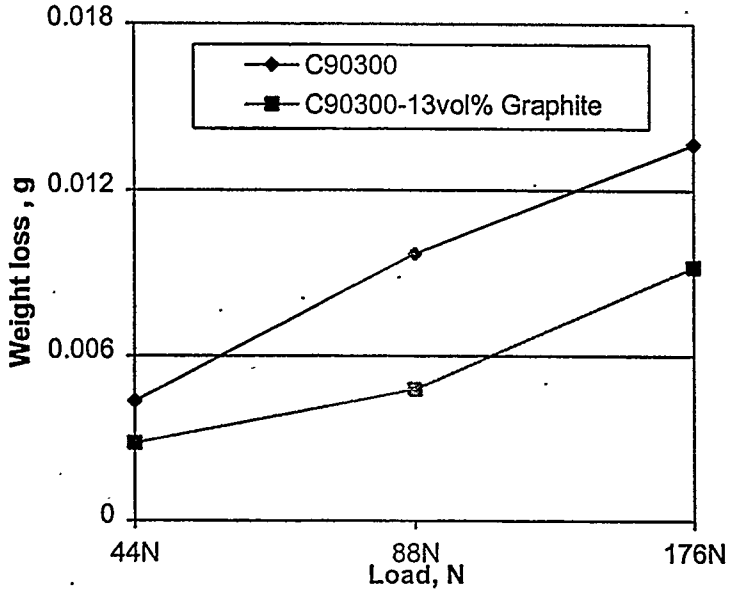

Figure 3.5.2. Variation of weight loss of the base alloy pin and centrifugally cast copper alloy C90300 originally containing 13vol% graphite particle (run against 1045 steel counterface) with applied load.

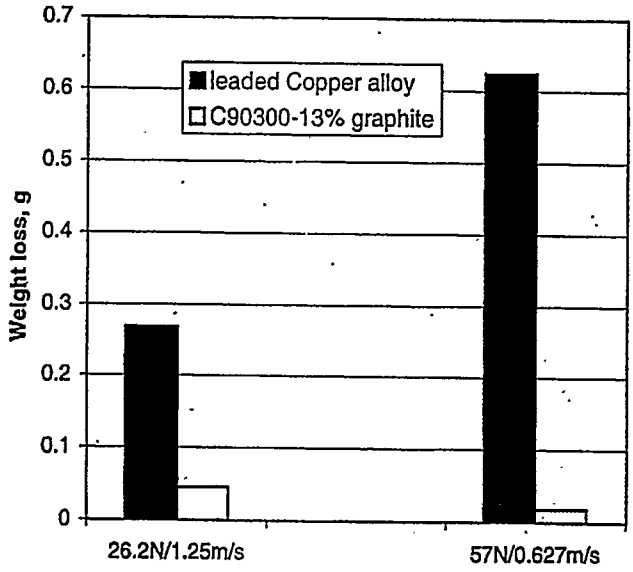

Figure 3.5.3. Variation of weight loss of centrifugally cast copper alloy C90300 originally containing 13vol% graphite particle and Leaded copper alloy run against 1045 steel counterface.

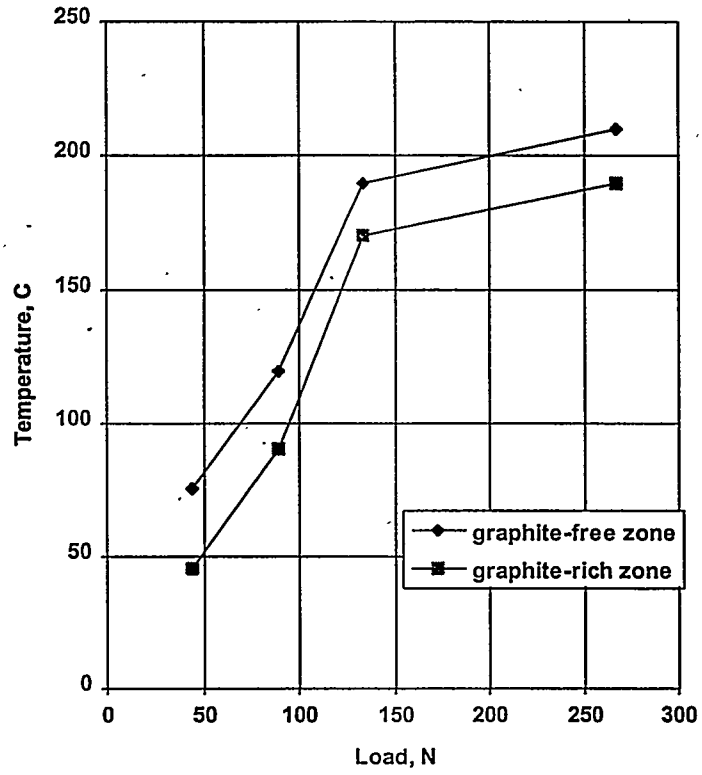

Fig.3.5.4. Variation of the temperature at the counterface with applied load for the graphite rich-zone and the graphite-free zone of centrifugally cast copper alloy originally containing 13 vol.% graphite after running against the cast iron for 5 minutes and at a speed of 1m/s.

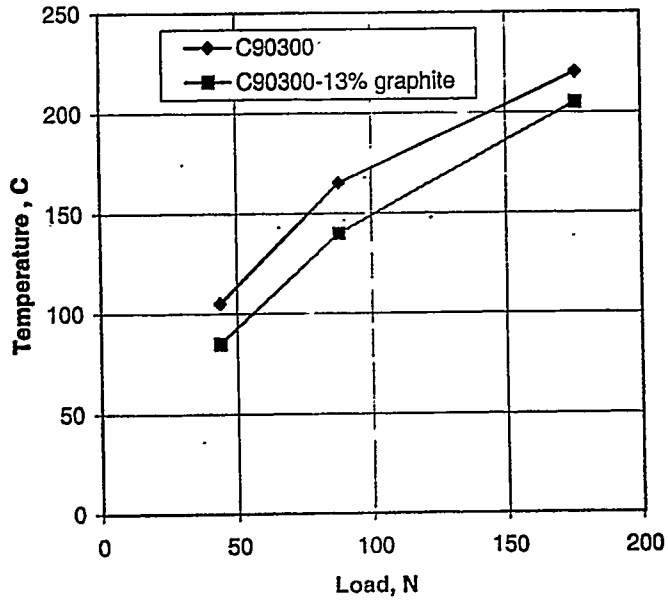

Figure 3.5.5. Variation of temperature at the counterface with applied load for the base alloyC90300 and centrifugally cast copper alloy C90300 originally containing 13vol% graphite particle

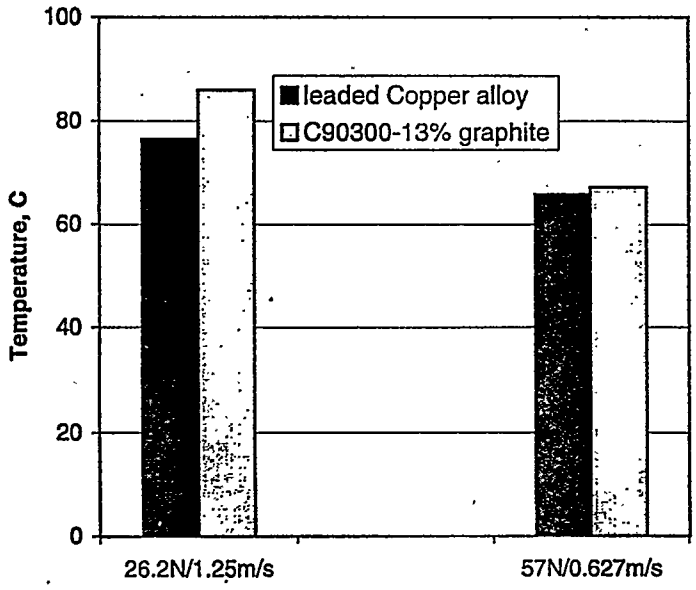

Figure 3.5.6. Variation of temperature at the counterface for Leaded copper alloy and centrifugally cast copper alloy C90300 originally containing 13vol% graphite particle tested under two different conditions.

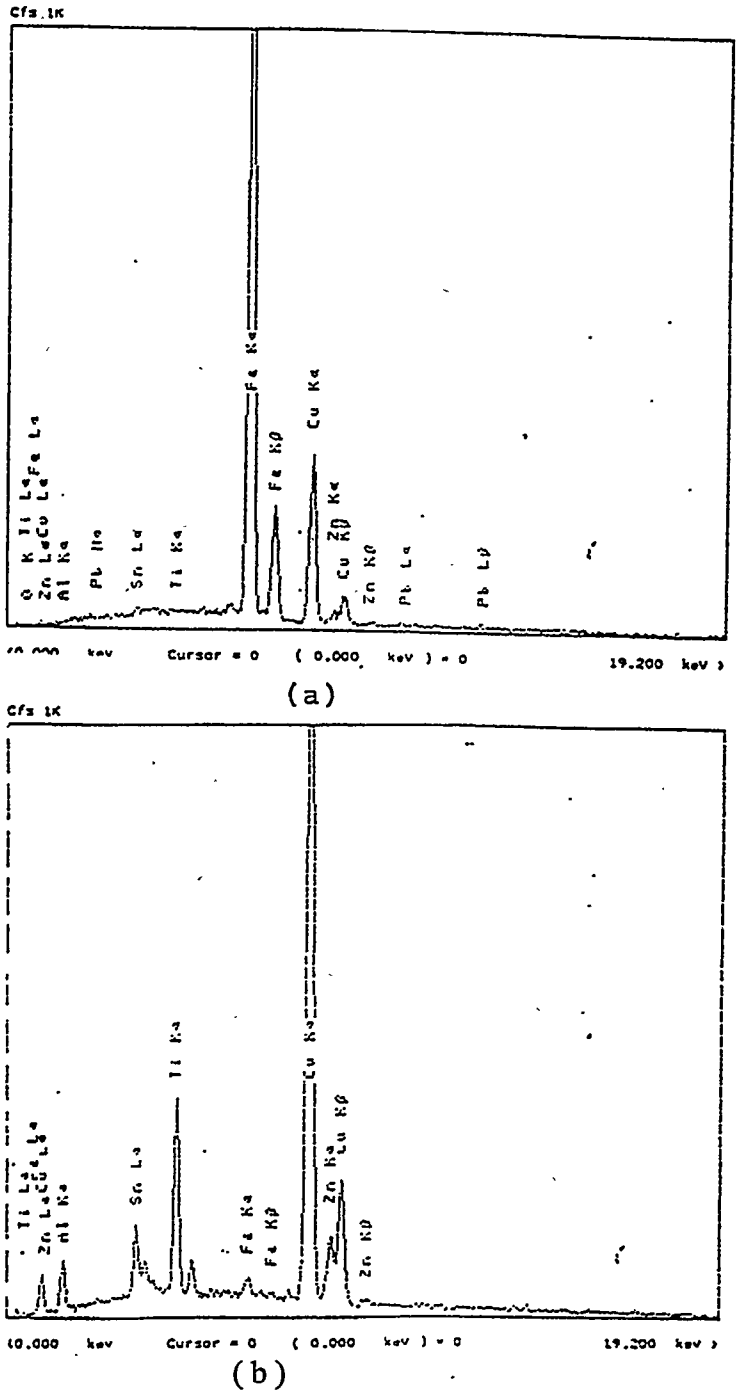

Figure 3.5.7. EDX analysis of the surface of the pin from (a) base alloy C90300 and (b) C90300-13% graphite, run against SAE 1045 steel counterface at 88N.

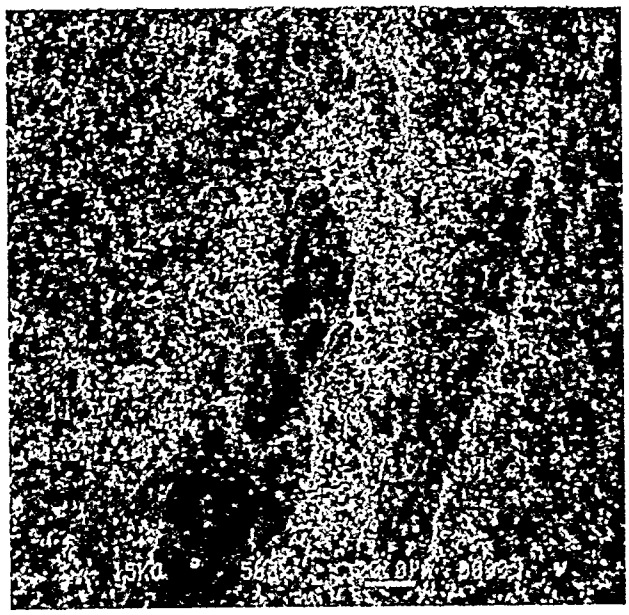

(a)

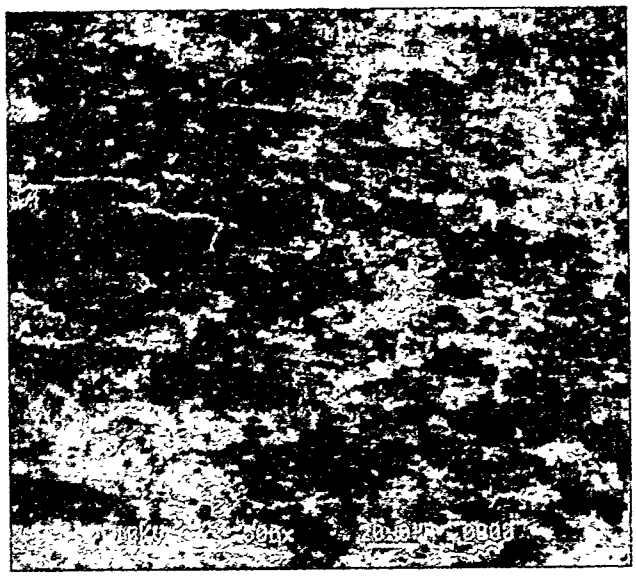

(b)

Figure 3.5.8. SEM picture of the surface of the pin from (a) base alloy C90300 and (b) C90300-13% graphite, run against SAE 1045 steel counterface at 44N.

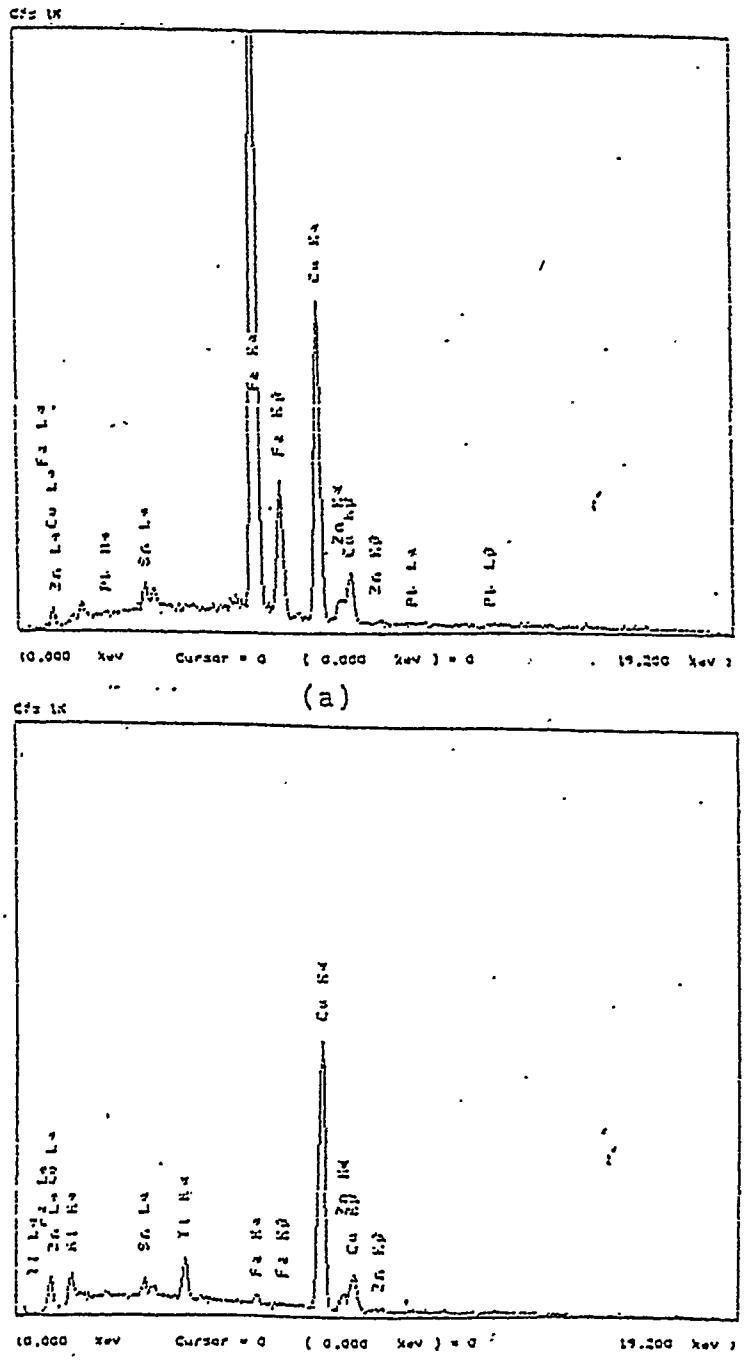

Figure 3.5.9. EDX analysis of the wear debris when pin from (a) base alloy C90300 and (b) C90300-13% graphite, ran against SAE 1045 steel counterface at 176N.

List of papers published under DOE project DE-FC07-931D13236

Conference Papers

1. P. K. Rohatgi, J. K. Kim, A. Saigal, J. Sobczak, and N. Sobczak, "Cast Lead-Free Copper Graphite Particle Composites for Bearing and Plumbing Applications", Proceedings of Process, Properties and Applications of Cast Metal Matrix Composites, Ed. by P.K.Rohatgi, ASM Materials Week Conference, Cincinnati, OH, 1996, pp. 271-288.

2. P. K. Rohatgi, J. Sobczak, N. Sobczak, and J. K. Kim, "Cast Copper Alloy Composite Reinforced with Graphite Particles', Proceedings of 2nd International Conference on Copper Alloys, Polish Academy Science, Poland, Nov., 1996, pp. 183-190.

3. P. K. Rohatgi, J. K. Kim, R. Guo, J. Sobczak, and D. Nath, "Tribological Properties of Centrifugally Cast Copper Alloy Containing Graphite Particles", Accepted for publication in Proceedings of Wear of Materials, ASM Materials Week Conference, Indianapolis, 1997.

4. P.K.Rohatgi, J. Sobczak, J.K.Kim, and N. Sobczak, "Casting of Copper alloys Containing Dispersed Graphite Particles in Rotating Molds", Proceedings of International Conference "Cast Composites '98", Poland, 1998, pp. 23-28.

5. M. Kestursatya, J.K. Kim, and P.K. Rohatgi, " Tribological Properties of Centrigually Cast Copper Alloy Containing Graphite Particles Against Steel", Presented at TMS Materials Week Conference, Rosemont, IL, 1998.

6. M. Kestursatya, J.K. Kim and P.K. Rohatgi, " Role of Surfaces on Tribological Behavior of Copper Graphite Composites", AVS Proceedings, June 14-17, 1999.

Published in Journals

1. P. K. Rohatgi, J. K. Kim, J. Sobczak, N. Sobczak, S. Ray, "Centrifugal Casting of Lead-Free Copper Graphite Alloys", AFS Transactions, 1996, vol. 104, pp. 1217-1222.

2. P.K.Rohatgi, J. Sobczak, N. Sobczak, and J. K. Kim, "Cast Copper Alloy Composites Reinforced with Graphite Particles," The Ores and Non-Ferrous Metals, Published by Polish Scientific Association of Metallurgical Engineers, No. R42/9, pp. 380-383, Poland, 1997.

3. J. K. Kim and P. K. Rohatgi, "Interaction Between Moving Solidification Front And Graphite Particles During Centrifugal Casting", Materials Science and Engineering, A244, 1998, pp. 168-177.

4. J. K. Kim and P. K. Rohatgi, "Formation of Graphite Rich Zone in Centrifugal Casting of Copper Alloy Graphite Composites", J. Materials Science, 33, 1998, pp. 2039-2045.

5. P.K.Rohatgi, J. K. Kim, J. Sobczak, and N. Sobczak, "Casting of Copper Alloys containing

Dispersed Graphite Particles in Rotating Molds", Foundryman, The institute of British Foundrymen, 1998, pp. 167-170.

6. J. K. Kim and P. K. Rohatgi, "Effect of Interactions Between Bubbles and Graphite Particles on Microstructure formed During Centrifugal Casting: Analytical Solution Part I", Metallurgical and Materials Transactions, 1999.

7. J. K. Kim and P. K. Rohatgi, "Effect of Interactions Between Bubbles and Graphite Particles on Microstructure formed During Centrifugal Casting: Experiments Part II", Metallurgical and Materials Transactions, 1999.

8 J. K. Kim and P. K. Rohatgi, "Tribological Properties of Centrifugally Cast Copper Alloy Graphite composites",to be submitted for publication in Metallurgical and Materials Transactions, 1999.